Soft two-meson-exchange nucleon-nucleon potentials.
II. One-pair and two-pair diagrams

Th.A. Rijken

Institute for Theoretical Physics, University of Nijmegen, Nijmegen, The Netherlands

V.G.J. Stoks*

Department of Physics, The Flinders University of South Australia, Bedford Park, South Australia 5042, Australia

Two-meson-exchange nucleon-nucleon potentials are derived where either one or both nucleons contains a pair vertex. Physically, the meson-pair vertices are meant to describe in an effective way (part of) the effects of heavy-meson exchange and meson-nucleon resonances. From the point of view of "duality," these two kinds of contribution are roughly equivalent. The various possibilities for meson pairs coupling to the nucleon are inspired by the chiral-invariant phenomenological Lagrangians that have appeared in the literature. The coupling constants are fixed using the linear σ model. We show that the inclusion of these two-meson exchanges gives a significant improvement over a potential model including only the standard one-boson exchanges.

13.75.Cs, 12.39.Pn, 21.30.-x

I. INTRODUCTION

In this second paper on two-meson-exchange potentials, we derive the contributions to the nucleon-nucleon potentials when either one or both nucleons contains a pair vertex. The corresponding "seagull" diagrams are labeled as one-pair and two-pair diagrams, and are depicted in Fig. 1. They are in a different class than the planar and crossed-box diagrams. The latter can be understood as the second-order contributions in a series expansion of multiple-meson exchanges and were calculated in the previous paper [1]. The two types of two-meson-exchange potentials presented here and in the previous paper [1] are part of our program to study the effect of two-meson exchanges in potential models and to extend the Nijmegen soft-core one-boson-exchange potential [2] to arrive at a new extended soft-core (ESC) nucleon-nucleon model, hereafter referred to as the ESC potential.

Our motivation for deriving the pair-meson potentials comes from "duality" [3, 4]. Since we do not explicitly include any contributions to the potentials coming from intermediate states with nucleon resonances, we have indicated in Fig. 2 how these resonances can be included via meson-pair contributions. According to "duality," the resonance contributions to the various meson-nucleon amplitudes can be described approximately by heavy-meson exchanges. Treating the heavy-meson propagators as constants, which should be adequate at low energies, leads directly to pair-meson exchanges. Hence, the pair-meson potentials can be viewed as the result of integrating out the heavy-meson and resonance degrees of freedom. We are less radical than Weinberg (see, e.g.,

Ref. [5]), in that we do not integrate out the degrees of freedom of the mesons with masses below 1 GeV.

The pairs we consider are $\pi\pi$, $\pi\rho$, $\pi\varepsilon$, and $\varepsilon\varepsilon$. They are inspired by the chiral-invariant phenomenological Lagrangians that have appeared in the literature, see for example [6, 7]. Here the $\varepsilon(760)$ scalar meson is treated as a very broad meson with a width of $\Gamma_\varepsilon \sim 640$ MeV [8]. The potential due to the exchange of a broad meson can be approximated by the sum of two potentials where each potential is due to the exchange of a stable meson [9, 10]. Because of the large width of the $\varepsilon(760)$, the low-mass pole in the two-pole approximation is rather small (~ 500 MeV). Hence, it is expected to contribute significantly to the two-meson potentials, which is the reason why we explicitly included the $\varepsilon\varepsilon$ pair potential. To emphasize the importance of the low-mass contribution, we will henceforth denote these scalar contributions to the pair potentials by $\pi\sigma$ and $\sigma\sigma$, where σ stands for the low-mass pole.

We neglect the contributions from the negative-energy states of the nucleons. We assume that at low energies a strong "nucleon-pair suppression" mechanism (i.e., suppression of the nucleon-antinucleon $N\overline{N}$ pairs) is operative. This is due to the compositeness and the large mass of the nucleons. Obviously, this is only valid in the low-energy regime. From relativity we know that nucleon-pair suppression cannot be absolute. However, we mention that it is very plausible from the point of view [11] of the nonrelativistic quark model (NRQM). Also, in the chiral quark-model picture [12] it is rather unlikely that $N\overline{N}$ pairs play a role in the low-energy region. Moreover, nucleon-pair suppression is substantiated by stud-

---

*Present address: TRIUMF, 4004 Wesbrook Mall, Vancouver, British Columbia, Canada V6T 2A3.

ies of the large N_c limit in QCD [13]. In this case, then, the Thomson limit is provided by the negative-energy contributions of the constituents, in particular the current quarks. A covariant description of this nucleon-pair suppression could very well be done by introducing off-mass-shell factors to the meson-nucleon-nucleon vertices. Instead of attempting such a covariant description in this paper, we simply neglect the transitions to the negative-energy states.

The paper is organized as follows. In Sec. II the meson-pair-exchange kernels are derived. We give the interaction Hamiltonians and the vertices in Pauli-spinor space, while the implementation of the Gaussian form factors is briefly indicated. In Sec. III we derive the one-pair and two-pair potentials. We then extend the calculations by including the $1/M$ corrections from the pseudovector vertex and from the nonadiabatic expansion of the energy denominators. The strength of the pair interactions can be estimated using the saturation with one-boson exchanges, but this involves some ambiguity in how to approximate the intermediate-boson propagator. In Sec. V we therefore choose to fix the pair coupling constants at their values as obtained in the linear σ model [14]. These values do not have to be taken exactly, of course, but they clearly suffice to demonstrate the improvements

that can be obtained when we include these pair interactions in a nucleon-nucleon potential model. Plots of the various pair potentials are then shown and discussed in Sec. VI. In this section we also compare this new ESC potential with the one-boson-exchange Nijm93 potential [15], demonstrating the significant improvement in the description of the scattering data that has been obtained by including the two-meson exchanges.

Finally, some details on parts of the calculation are collected in two appendices, while the coordinate-space pair potentials are given explicitly in Appendix C.

II. PAIR-MESON-EXCHANGE KERNEL

The fourth-order two-meson-exchange kernel is derived following the procedure as discussed in the previous paper [1], which closely follows an earlier publication [16], where we derived the soft two-pion-exchange potential. For details and definitions we refer to these two references.

Rather than repeating the derivation again, we here immediately proceed to give the one-pair and two-pair kernels. Introducing subscripts $1P$ and $2P$, the one-pair kernel is given by

$$K_{1P}(\mathbf{p}',\mathbf{p}|W)_{a'b';ab} = -(2\pi)^{-2}[W - \mathcal{W}(\mathbf{p}')]\,[W - \mathcal{W}(\mathbf{p})]\sum_{a'',b''}\int dp_0' \int dp_0 \int dk_{10} \int dk_{20} \int d\mathbf{k}_1 \int d\mathbf{k}_2 i(2\pi)^{-4}$$

$$\times \delta^4(p'-p-k_1-k_2)[k_2^2 - m_2^2 + i\delta]^{-1}[F_W^{(a')}(\mathbf{p}',p_0')F_W^{(b')}(-\mathbf{p}',-p_0')]^{-1}\{[\Gamma_{j,i}(\mathbf{p}',p_0';\mathbf{p},p_0)]$$

$$\times [\Gamma_j F_W^{-1}(-\mathbf{p}-\mathbf{k}_1,-p_0-k_{10})\Gamma_i]^{(b'')} + [\Gamma_j F_W^{-1}(\mathbf{p}+\mathbf{k}_1,p_0+k_{10})\Gamma_i]^{(a'')}$$

$$\times [\Gamma_{j,i}(-\mathbf{p}',-p_0';-\mathbf{p},-p_0)]\}\,[F_W^{(a)}(\mathbf{p},p_0)F_W^{(b)}(-\mathbf{p},-p_0)]^{-1}[k_1^2 - m_1^2 + i\delta]^{-1}, \tag{2.1}$$

whereas the two-pair kernel is given by

$$K_{2P}(\mathbf{p}',\mathbf{p}|W)_{a'b';ab} = -(2\pi)^{-2}[W - \mathcal{W}(\mathbf{p}')]\,[W - \mathcal{W}(\mathbf{p})]\int dp_0' \int dp_0 \int dk_{10} \int dk_{20} \int d\mathbf{k}_1 \int d\mathbf{k}_2 i(2\pi)^{-4}$$

$$\times \delta^4(p'-p-k_1-k_2)[k_2^2 - m_2^2 + i\delta]^{-1}[F_W^{(a')}(\mathbf{p}',p_0')F_W^{(b')}(-\mathbf{p}',-p_0')]^{-1}\{[\Gamma_{j,i}(\mathbf{p}',p_0';\mathbf{p},p_0)]$$

$$\times [\Gamma_{j,i}(-\mathbf{p}',-p_0';-\mathbf{p},-p_0)]\}\,[F_W^{(a)}(\mathbf{p},p_0)F_W^{(b)}(-\mathbf{p},-p_0)]^{-1}[k_1^2 - m_1^2 + i\delta]^{-1}. \tag{2.2}$$

Here m_1 and m_2 denote the two meson masses, Γ_i and Γ_j denote the nucleon-nucleon-meson vertices, and $\Gamma_{j,i}$ denotes the nucleon-nucleon-meson-meson vertex; they follow from the interaction Hamiltonians (see below). Because we only consider nucleons in the intermediate state, we have $a = a' = a'' = N$ and $b = b' = b'' = N$. Note that the first term between the curly brackets in the one-pair kernel corresponds to having the pair vertex on the first nucleon (hence, no label a''), and the second term to having the pair vertex on the other nucleon (no label b'').

From the explicit expressions (2.1) and (2.2), it is clear that one can perform the integration over the energy variables p_0', p_0, k_{10}, and k_{20}. The execution of these inte-

grals is quite similar to those worked out explicitly in Ref. [16], and so are the results. Details are given in Appendix A. In the case of the one-pair diagrams, we have taken the diagram where the meson-pair vertex is on line a.

In the adiabatic approximation, i.e., $E(\mathbf{p}) \approx M$, the energy denominators of the various time-ordered diagrams are

$$D_a^{(1)}(\omega_1,\omega_2) = \frac{1}{2\omega_1\omega_2}\frac{1}{\omega_2(\omega_1+\omega_2)},$$

$$D_b^{(1)}(\omega_1,\omega_2) = \frac{1}{2\omega_1^2\omega_2^2},$$

$$D_c^{(1)}(\omega_1, \omega_2) = \frac{1}{2\omega_1\omega_2} \frac{1}{\omega_1(\omega_1+\omega_2)},$$

$$D^{(2)}(\omega_1, \omega_2) = -\frac{1}{2\omega_1\omega_2} \frac{1}{\omega_1+\omega_2}. \tag{2.3}$$

Here we have labeled the three time-ordered one-pair graphs by a, b, and c, which correspond, respectively, to the diagrams depicted in Fig. 3. However, since we always have to add the contribution from the "mirror" graphs anyway (i.e., with the pair vertex at line b), we have already included the resulting factor of 2 in the $D^{(1)}$ energy denominators of Eq. (2.3). The two time-ordered graphs for the two-pair diagrams are each other's "mirror" graphs. In most cases the vertices do not explicitly depend on the time ordering and we can add the three time-ordered one-pair energy denominators to give

$$D^{(1)}(\omega_1, \omega_2) = D_a^{(1)} + D_b^{(1)} + D_c^{(1)} = \frac{1}{\omega_1^2 \omega_2^2}. \tag{2.4}$$

Before we can proceed and calculate the pair-meson potentials, we have to define the nucleon-nucleon-meson (NNm) and nucleon-nucleon-meson-meson (NNm_1m_2) Hamiltonians. For point couplings the nucleon-nucleon-meson Hamiltonians are

$$\mathcal{H}_P = \frac{f_P}{m_\pi} \bar\psi \gamma_5 \gamma_\mu \boldsymbol{\tau} \psi \cdot \partial^\mu \boldsymbol{\phi}_P, \tag{2.5a}$$

$$\mathcal{H}_V = g_V \bar\psi \gamma_\mu \boldsymbol{\tau} \psi \cdot \boldsymbol{\phi}_V^\mu - \frac{f_V}{2M} \bar\psi \sigma_{\mu\nu} \boldsymbol{\tau} \psi \cdot \partial^\nu \boldsymbol{\phi}_V^\mu, \tag{2.5b}$$

$$\mathcal{H}_S = g_S \bar\psi \boldsymbol{\tau} \psi \cdot \boldsymbol{\phi}_S, \tag{2.5c}$$

where ϕ denotes the pseudovector-, vector-, and scalar-meson fields, respectively. For the isospin $I = 0$ mesons, the isospin Pauli matrices $\boldsymbol{\tau}$ are absent.

For the phenomenological meson-pair interactions, the Hamiltonians are

$$\mathcal{H}_S = \bar\psi\psi \left[g_{(\pi\pi)_0} \boldsymbol{\pi}\cdot\boldsymbol{\pi} + g_{(\sigma\sigma)}\sigma^2 \right]/m_\pi, \tag{2.6a}$$

$$\mathcal{H}_V = g_{(\pi\pi)_1} \bar\psi \gamma_\mu \boldsymbol{\tau} \psi \cdot (\boldsymbol{\pi}\times\partial^\mu\boldsymbol{\pi})/m_\pi^2$$
$$- \frac{f_{(\pi\pi)_1}}{2M} \bar\psi \sigma_{\mu\nu} \boldsymbol{\tau}\psi \partial^\nu \cdot (\boldsymbol{\pi}\times\partial^\mu\boldsymbol{\pi})/m_\pi^2, \tag{2.6b}$$

$$\mathcal{H}_A = g_{(\pi\rho)_1} \bar\psi \gamma_5 \gamma_\mu \boldsymbol{\tau}\psi \cdot (\boldsymbol{\pi}\times\boldsymbol{\rho}^\mu)/m_\pi, \tag{2.6c}$$

$$\mathcal{H}_P = g_{(\pi\sigma)} \bar\psi \gamma_5 \gamma_\mu \boldsymbol{\tau}\psi \cdot (\boldsymbol{\pi}\partial^\mu\sigma - \sigma\partial^\mu\boldsymbol{\pi})/m_\pi^2. \tag{2.6d}$$

The transition from Dirac spinors to Pauli spinors is reviewed in Appendix C of [16]. Following this reference and keeping only terms up to order $1/M$, we find that

the vertex operators in Pauli-spinor space for the NNm vertices are given by

$$\bar u(\mathbf{p}')\Gamma_P^{(1)}u(\mathbf{p}) = -i\frac{f_P}{m_\pi}\left[\boldsymbol{\sigma}_1\cdot\mathbf{k} \pm \frac{\omega}{2M}\boldsymbol{\sigma}_1\cdot(\mathbf{p}'+\mathbf{p})\right], \tag{2.7a}$$

$$\bar u(\mathbf{p}')\Gamma_V^{(1)}u(\mathbf{p})$$
$$= g_V\left[\phi_V^0 - \frac{1}{2M}\{(\mathbf{p}'+\mathbf{p}) + i(1+\kappa_V)\boldsymbol{\sigma}_1\times\mathbf{k}\}\cdot\boldsymbol{\phi}_V\right], \tag{2.7b}$$

$$\bar u(\mathbf{p}')\Gamma_S^{(1)}u(\mathbf{p}) = g_S, \tag{2.7c}$$

where we defined $\mathbf{k} = \mathbf{p}' - \mathbf{p}$ and $\kappa_V = f_V/g_V$. In the pseudovector vertex, the upper (lower) sign stands for creation (absorption) of the pion at the vertex. Similarly, the NNm_1m_2 vertices result in

$$\bar u(\mathbf{p}')\Gamma_S^{(2)}u(\mathbf{p}) = g_{(\pi\pi)_0}/m_\pi \quad \text{and} \quad g_{(\sigma\sigma)}/m_\pi, \tag{2.8a}$$

$$\bar u(\mathbf{p}')\Gamma_V^{(2)}u(\mathbf{p}) = ig_{(\pi\pi)_1}\left[(\pm\omega_1\mp\omega_2) + \frac{1}{M}\{\mathbf{q}\cdot(\mathbf{k}_1-\mathbf{k}_2) \right.$$
$$\left. -(1+\kappa_1)\boldsymbol{\sigma}_1\cdot(\mathbf{k}_1\times\mathbf{k}_2)\}\right]/m_\pi^2, \tag{2.8b}$$

$$\bar u(\mathbf{p}')\Gamma_A^{(2)}u(\mathbf{p}) = g_{(\pi\rho)_1}\left[\boldsymbol{\sigma}_1\cdot\boldsymbol{\rho} - \frac{1}{M}\boldsymbol{\sigma}_1\cdot\mathbf{q}\rho^0\right]/m_\pi, \tag{2.8c}$$

$$\bar u(\mathbf{p}')\Gamma_P^{(2)}u(\mathbf{p}) = ig_{(\pi\sigma)}\left[\boldsymbol{\sigma}_1\cdot(\mathbf{k}_1-\mathbf{k}_2) \right.$$
$$\left. - \frac{1}{M}\boldsymbol{\sigma}_1\cdot\mathbf{q}(\pm\omega_1\mp\omega_2)\right]/m_\pi^2, \tag{2.8d}$$

where $\mathbf{q} = \frac{1}{2}(\mathbf{p}' + \mathbf{p})$ and $\kappa_1 = (f/g)_{(\pi\pi)_1}$. Again, the upper (lower) sign in front of ω_1 and ω_2 refers to creation (absorption) of the meson at the vertex. For both the NNm and NNm_1m_2 vertices, the expressions for $\bar u(-\mathbf{p}')\Gamma u(-\mathbf{p})$ are trivially obtained by substituting $(\mathbf{p}', \mathbf{p}, \mathbf{k}_i, \omega_i, \boldsymbol{\sigma}_1) \to (-\mathbf{p}', -\mathbf{p}, -\mathbf{k}_i, \omega_i, \boldsymbol{\sigma}_2)$.

The generalization of the interaction kernels to the case with a Gaussian (or any other) form factor has been treated and explained in [16]. We make the substitution

$$[k^2 - m^2 + i\delta]^{-1} \longrightarrow \int_0^\infty d\mu^2 \frac{\rho(\mu^2)}{k^2 - \mu^2 + i\delta}, \tag{2.9}$$

for each meson-exchange line in the Feynman diagrams. Here, $\rho(\mu^2)$ is the spectral function, representing the form factors involved in meson exchange. At low and medium energy, we have to a very good approximation $t = k^2 \approx -\mathbf{k}^2 < 0$, and so for spacelike momentum transfers we can use Gaussian form factors $F(\mathbf{k}^2) = \exp(-\mathbf{k}^2/\Lambda^2)$, where Λ denotes the cutoff mass. The Gaussian form factor is introduced by the substitution

$$\int_0^\infty d\mu^2 \frac{\rho(\mu^2)}{\mathbf{k}^2 + \mu^2} \longrightarrow \frac{F(\mathbf{k}^2)}{\mathbf{k}^2 + m^2}. \qquad (2.10)$$

The NNm and NNm_1m_2 vertices have different form factors. We will use

$$F_{NNm_1m_2}(\mathbf{k}_1, \mathbf{k}_2) = \exp(-\mathbf{k}_1^2/2\Lambda_1^2)\exp(-\mathbf{k}_2^2/2\Lambda_2^2),$$

$$F_{NNm}(\mathbf{k}^2) = \exp(-\mathbf{k}^2/2\Lambda_m^2), \qquad (2.11)$$

where Λ_1 and Λ_2 are the form factor masses for mesons m_1 and m_2, respectively. A motivation for this prescription could be that in "duality" the structure of the NNm_1m_2 vertex is either saturated by heavy mesons or meson-nucleon resonances. In this last case, assuming that the meson-nucleon resonance transitions all have roughly the same (inelastic) form factor, the form (2.11) is a natural one.

III. MESON-PAIR POTENTIALS

In this paper we restrict ourselves mainly to the pion-meson pair potentials. The only exception is the $\sigma\sigma$-pair potential, but the derivation of the potential for any other combination of two mesons will be straightforward. Here σ stands for the low-mass pole in the two-pole approximation [9, 10] of the broad $\varepsilon(760)$ scalar meson. (At this point it might be worthwhile to mention that in the previous paper [1] we refrained from evaluating the $\sigma\sigma$ planar and crossed-box contributions. The reason for this is that the leading-order contribution of a potential due to the exchange of two isoscalar-scalar mesons is identically zero.) In the description of the pion-meson pair potentials we always assign the index 1 to the pion, and the index 2 to the other meson, which can be a pion as well.

Armed with the Pauli-spinor vertices given in the previous section, it is now straightforward to derive the one-pair and two-pair potentials. They can be succinctly written as

$$
\begin{aligned}
V_{\text{pair}}^{(n)}(\alpha\beta) = & C^{(n)}(\alpha\beta)g^{(n)}(\alpha\beta)\iint \frac{d^3k_1 d^3k_2}{(2\pi)^6} \\
& \times e^{i(\mathbf{k}_1+\mathbf{k}_2)\cdot\mathbf{r}} F_\alpha(\mathbf{k}_1^2)F_\beta(\mathbf{k}_2^2) \\
& \times \sum_p O_{\alpha\beta,p}^{(n)}(\mathbf{k}_1,\omega_1;\mathbf{k}_2,\omega_2)D_p^{(n)}(\omega_1,\omega_2),
\end{aligned}
$$
$$(3.1)$$

where the index n distinguishes one-pair ($n = 1$) and two-pair ($n = 2$) meson-pair exchange, and $(\alpha\beta)$ refers to the particular meson pair that is being exchanged. The product of the coupling constants in the two cases is given by

$$g^{(1)}(\alpha\beta) = g_{(\alpha\beta)}g_{NN\alpha}g_{NN\beta},$$

$$g^{(2)}(\alpha\beta) = g_{(\alpha\beta)}^2, \qquad (3.2)$$

with appropriate powers of m_π, depending on the definition of the Hamiltonians. The energy denominators $D_p^{(n)}$ are given in Eq. (2.3), with the index p labeling the different time-ordered processes. Finally, the momentum-dependent operators $O_{\alpha\beta,p}^{(n)}$ are given in Tables I and II. For completeness, these tables also contain the isospin factors $C^{(n)}(\alpha\beta)$ as derived in Appendix B. The momentum operators for $(\pi\pi)_0$ and $(\pi\pi)_1$ both contain a term antisymmetric in $\mathbf{k}_1 \leftrightarrow \mathbf{k}_2$. They only contribute when we make the nonadiabatic expansion (see Sec. IV). In the leading-order potential (3.1) they drop out when we integrate over $\mathbf{k}_1$ and $\mathbf{k}_2$.

The time-ordering label p in Eq. (3.1) is only of interest for the $(\pi\pi)_1$ one-pair potential, where we have an explicit (ω_1, ω_2) dependence in $O_{\pi\pi,p}^{(1)}$. For all other one-pair potentials we have the same energy denominator $D^{(1)}(\omega_1, \omega_2)$ as given in Eq. (2.4), and we can drop the p index in $O_{\alpha\beta,p}^{(1)}$. For $(\alpha\beta) = (\pi\pi)_1$, the three time-ordered diagrams contribute as

$$
\begin{aligned}
(-\omega_1 + \omega_2)D_a^{(1)} + (\omega_1 + \omega_2)&D_b^{(1)} + (\omega_1 - \omega_2)D_c^{(1)} \\
&= \frac{2}{\omega_1\omega_2(\omega_1 + \omega_2)}.
\end{aligned}
$$

Similarly, the two-pair potentials are all seen to have the energy denominator $D^{(2)}$ of Eq. (2.3), where the additional $(\omega_1 - \omega_2)^2$ dependence in $O_{\alpha\beta}^{(2)}$ for $(\pi\pi)_1$ can be rewritten as

$$(\omega_1 - \omega_2)^2 D^{(2)} = -\frac{1}{2\omega_1} - \frac{1}{2\omega_2} + \frac{2}{\omega_1 + \omega_2}.$$

The evaluation of the momentum integrations can now readily be performed using the methods given in [1, 16]. There it was shown that the full separation of the $\mathbf{k}_1$ and $\mathbf{k}_2$ dependence of the Fourier integrals can be achieved in all cases using the λ-integral representation. Starting out from Eq. (3.1), this procedure gives the following generic form of the potentials in coordinate space:

$$
\begin{aligned}
V_{\text{pair}}^{(n)}(\alpha\beta) = & C^{(n)}(\alpha\beta)g^{(n)}(\alpha\beta) \lim_{\mathbf{r}_1,\mathbf{r}_2\to\mathbf{r}} \\
& \times O_{\alpha\beta}^{(n)}(-i\boldsymbol{\nabla}_1,\omega_1;-i\boldsymbol{\nabla}_2,\omega_2)B_{\alpha\beta}^{(n)}(r_1,r_2).
\end{aligned}
$$
$$(3.3)$$

The different functions $B_{\alpha\beta}(r_1, r_2)$ that occur in this expression involve the functions $I_2(m, r)$ as defined in Ref. [16], $I_0(\Lambda, r)$ as defined in Ref. [1], and the integrals

$$B_{0,0}(m_\alpha, r_1; m_\beta, r_2) = \frac{2}{\pi}\int_0^\infty d\lambda\, \lambda^2 F_\alpha(\lambda, r_1)F_\beta(\lambda, r_2),$$

$$B_{1,1}(m_\alpha, r_1; m_\beta, r_2) = \frac{2}{\pi}\int_0^\infty d\lambda\, F_\alpha(\lambda, r_1)F_\beta(\lambda, r_2), \quad (3.4)$$

where

4

$$F_\alpha(\lambda, r) = e^{-\lambda^2/\Lambda_\alpha^2} I_2(\sqrt{m_\alpha^2 + \lambda^2}, r). \qquad (3.5)$$

The differentiation operations needed in Eq. (3.3) are listed in Appendix A of the previous paper [1], and the resulting coordinate-space potentials are here given explicitly in Appendix C.

IV. $1/M$ CORRECTIONS

The nonadiabatic correction from the $1/M$ expansion of the energy denominators is explained in Ref. [16]. The expansion of the energy denominator involves a momentum dependence which can be rewritten in the form $[\mathbf{k}_1 \cdot \mathbf{k}_2 - \mathbf{q} \cdot (\mathbf{k}_1 - \mathbf{k}_2)]/2M$.

Taking out the momentum-dependent factor, the one-pair energy denominators of Eq. (2.3) give rise to the energy denominators

$$D_a^{\mathrm{na}}(\omega_1, \omega_2) = \frac{1}{2\omega_1\omega_2} \frac{1}{\omega_2^2(\omega_1 + \omega_2)},$$

$$D_b^{\mathrm{na}}(\omega_1, \omega_2) = \frac{1}{2\omega_1\omega_2} \left(\frac{1}{\omega_1^2\omega_2} + \frac{1}{\omega_1\omega_2^2} \right),$$

$$D_c^{\mathrm{na}}(\omega_1, \omega_2) = \frac{1}{2\omega_1\omega_2} \frac{1}{\omega_1^2(\omega_1 + \omega_2)}. \qquad (4.1)$$

Again, the time ordering is only of importance in the $(\pi\pi)_1$ potential, where the contributions sum up to

$$D_{(\pi\pi)_1}^{\mathrm{na}} = \frac{2}{\omega_1^2\omega_2^2}. \qquad (4.2)$$

In all other cases the three energy denominators of Eq. (4.1) can be summed directly, yielding

$$D^{\mathrm{na}} = \frac{1}{\omega_1^2\omega_2^2} \left[\frac{1}{\omega_1} + \frac{1}{\omega_2} - \frac{1}{\omega_1 + \omega_2} \right], \qquad (4.3)$$

which gives rise to a coordinate-space function of the form

$$B_{\alpha\beta}^{\mathrm{na}}(r_1, r_2) = \frac{2}{\pi} \int_0^\infty \frac{d\lambda}{\lambda^2} [I_2(m_\alpha, r_1) I_2(m_\beta, r_2) \\ - F_\alpha(\lambda, r_1) F_\beta(\lambda, r_2)]. \qquad (4.4)$$

The energy denominators $D^{\mathrm{na}}(\omega_1, \omega_2)$ are symmetric under interchanges of labels 1 and 2, and so the term proportional to $\mathbf{q} \cdot (\mathbf{k}_1 - \mathbf{k}_2)$ will only contribute in combination with the antisymmetric terms in $O^{(1)}(\mathbf{k}_1, \omega_1; \mathbf{k}_2 \omega_2)$; i.e., in $(\pi\pi)_0$ and $(\pi\pi)_1$. We find

$$V^{\mathrm{na}}[(\pi\pi)_0] = -\frac{g_{(\pi\pi)_0}}{m_\pi} \left(\frac{f_{NN\pi}}{m_\pi} \right)^2 \frac{3}{M} \iint \frac{d^3k_1 d^3k_2}{(2\pi)^6} e^{i(\mathbf{k}_1 + \mathbf{k}_2) \cdot \mathbf{r}} F_\pi(\mathbf{k}_1^2) F_\pi(\mathbf{k}_2^2)$$
$$\times \left[(\mathbf{k}_1 \cdot \mathbf{k}_2)^2 + \tfrac{i}{2} \mathbf{q} \cdot (\mathbf{k}_1 - \mathbf{k}_2)(\boldsymbol{\sigma}_1 + \boldsymbol{\sigma}_2) \cdot (\mathbf{k}_1 \times \mathbf{k}_2) \right] D^{\mathrm{na}}(\omega_1, \omega_2), \qquad (4.5)$$

$$V^{\mathrm{na}}[(\pi\pi)_1] = -(\boldsymbol{\tau}_1 \cdot \boldsymbol{\tau}_2) \frac{g_{(\pi\pi)_1}}{m_\pi^2} \left(\frac{f_{NN\pi}}{m_\pi} \right)^2 \frac{1}{M} \iint \frac{d^3k_1 d^3k_2}{(2\pi)^6} e^{i(\mathbf{k}_1 + \mathbf{k}_2) \cdot \mathbf{r}} F_\pi(\mathbf{k}_1^2) F_\pi(\mathbf{k}_2^2)$$
$$\times \left[(\mathbf{k}_1 \cdot \mathbf{k}_2)^2 + \tfrac{i}{2} \mathbf{q} \cdot (\mathbf{k}_1 - \mathbf{k}_2)(\boldsymbol{\sigma}_1 + \boldsymbol{\sigma}_2) \cdot (\mathbf{k}_1 \times \mathbf{k}_2) \right] \frac{2}{\omega_1^2\omega_2^2}, \qquad (4.6)$$

$$V^{\mathrm{na}}[(\sigma\sigma)] = \frac{g_{(\sigma\sigma)}}{m_\pi} \frac{g_{NN\sigma}^2}{M} \iint \frac{d^3k_1 d^3k_2}{(2\pi)^6} e^{i(\mathbf{k}_1 + \mathbf{k}_2) \cdot \mathbf{r}} F_\sigma(\mathbf{k}_1^2) F_\sigma(\mathbf{k}_2^2)(\mathbf{k}_1 \cdot \mathbf{k}_2) D^{\mathrm{na}}(\omega_1, \omega_2), \qquad (4.7)$$

$$V^{\mathrm{na}}[(\pi\sigma)] = -(\boldsymbol{\tau}_1 \cdot \boldsymbol{\tau}_2) \frac{g_{(\pi\sigma)}}{m_\pi^2} \frac{f_{NN\pi}}{m_\pi} \frac{g_{NN\sigma}}{M} \iint \frac{d^3k_1 d^3k_2}{(2\pi)^6} e^{i(\mathbf{k}_1 + \mathbf{k}_2) \cdot \mathbf{r}} F_\pi(\mathbf{k}_1^2) F_\sigma(\mathbf{k}_2^2)$$
$$\times (\mathbf{k}_1 \cdot \mathbf{k}_2) \left[\boldsymbol{\sigma}_1 \cdot \mathbf{k}_1 \boldsymbol{\sigma}_2 \cdot \mathbf{k}_1 - \tfrac{1}{2}(\boldsymbol{\sigma}_1 \cdot \mathbf{k}_1 \boldsymbol{\sigma}_2 \cdot \mathbf{k}_2 + \boldsymbol{\sigma}_1 \cdot \mathbf{k}_2 \boldsymbol{\sigma}_2 \cdot \mathbf{k}_1) \right] D^{\mathrm{na}}(\omega_1, \omega_2), \qquad (4.8)$$

where we substituted the isospin dependence and the coupling constants.

The pseudovector vertex gives rise to $1/M$ terms as shown in Eq. (2.7a). Taking into account the different time orderings and discarding the terms antisymmetric under interchange of $\mathbf{k}_1 \leftrightarrow \mathbf{k}_2$, we find the contributions

$$V^{\mathrm{pv}}[(\pi\pi)_0] = \frac{g_{(\pi\pi)_0}}{m_\pi} \left(\frac{f_{NN\pi}}{m_\pi} \right)^2 \frac{3}{M} \iint \frac{d^3k_1 d^3k_2}{(2\pi)^6} e^{i(\mathbf{k}_1 + \mathbf{k}_2) \cdot \mathbf{r}} F_\pi(\mathbf{k}_1^2) F_\pi(\mathbf{k}_2^2)$$
$$\times [\mathbf{k}_1^2 + \mathbf{k}_2^2 - i(\boldsymbol{\sigma}_1 + \boldsymbol{\sigma}_2) \cdot (\mathbf{k}_1 + \mathbf{k}_2) \times \mathbf{q}] \frac{1}{\omega_1\omega_2(\omega_1 + \omega_2)}, \qquad (4.9)$$

$$V^{\mathrm{pv}}[(\pi\pi)_1] = (\boldsymbol{\tau}_1\cdot\boldsymbol{\tau}_2)\frac{g_{(\pi\pi)_1}}{m_\pi^2}\left(\frac{f_{NN\pi}}{m_\pi}\right)^2\frac{1}{M}\iint\frac{d^3k_1 d^3k_2}{(2\pi)^6}\,e^{i(\mathbf{k}_1+\mathbf{k}_2)\cdot\mathbf{r}}F_\pi(\mathbf{k}_1^2)F_\pi(\mathbf{k}_2^2)$$
$$\times\left[\left(\frac{\mathbf{k}_1^2}{\omega_1^2}+\frac{\mathbf{k}_2^2}{\omega_2^2}\right)-i(\boldsymbol{\sigma}_1+\boldsymbol{\sigma}_2)\cdot\left(\frac{\mathbf{k}_1}{\omega_1^2}+\frac{\mathbf{k}_2}{\omega_2^2}\right)\times\mathbf{q}\right], \tag{4.10}$$

$$V^{\mathrm{pv}}[(\pi\sigma)] = -(\boldsymbol{\tau}_1\cdot\boldsymbol{\tau}_2)\frac{g_{(\pi\sigma)}}{m_\pi^2}\frac{f_{NN\pi}}{m_\pi}\frac{g_{NN\sigma}}{M}\iint\frac{d^3k_1 d^3k_2}{(2\pi)^6}\,e^{i(\mathbf{k}_1+\mathbf{k}_2)\cdot\mathbf{r}}F_\pi(\mathbf{k}_1^2)F_\sigma(\mathbf{k}_2^2)$$
$$\times\left[\boldsymbol{\sigma}_1\cdot\mathbf{k}_2\boldsymbol{\sigma}_2\cdot\mathbf{k}_2-\tfrac{1}{2}(\boldsymbol{\sigma}_1\cdot\mathbf{k}_1\boldsymbol{\sigma}_2\cdot\mathbf{k}_2+\boldsymbol{\sigma}_1\cdot\mathbf{k}_2\boldsymbol{\sigma}_2\cdot\mathbf{k}_1)\right]\frac{1}{\omega_1\omega_2(\omega_1+\omega_2)}. \tag{4.11}$$

V. THEORETICAL CONSTRAINTS ON PAIR COUPLING CONSTANTS

In principle, each of the pair-meson potentials contains a free parameter, the pair-meson coupling constant. A possible way to fix the values for the pair-meson coupling constants is to assume that the coupling of a meson pair $(\alpha\beta)$ to a nucleon is dominated by an intermediate boson H. We can then relate the pair coupling constant $g_{(\alpha\beta)}$ to the meson-decay and meson-nucleon coupling constants $g_{H\alpha\beta}$ and g_{NNH}, respectively. The relevant nucleon-nucleon-meson and meson-decay Lagrangians can then be obtained by extending the linear σ model [14] with vector and axial-vector mesons; see, for example, Refs. [17, 18, 19].

Meson saturation is graphically presented in Fig. 4. Because of the additional meson propagator and the meson-decay vertex, we find the relation

$$g_{(\alpha\beta)} \approx -\frac{(-)^S}{m_H^2}g_{NNH}g_{H\alpha\beta}, \tag{5.1}$$

with appropriate powers of meson masses, depending on the actual form of the meson-pair and meson-decay Hamiltonians. Here S denotes the spin of the intermediate meson H and we assumed that m_H^2 is much larger than the momentum-transfer squared. However, for the $(\pi\pi)_1$ and $(\pi\pi)_0$ pairs the decay can proceed via the ρ and σ mesons, respectively. These are substantially lighter than 1 GeV, and so we are faced with the difficult task of finding a suitable average momentum squared to approximate $(\mathbf{k}^2+m_H^2)$. Another problem is that a specific meson pair might be the decay product of a range of different mesons, and so Eq. (5.1) becomes a sum over mesons H_i, confusing the issue even further. Alternatively, we can also use the linear σ model to generate the pair vertices explicitly, which we shall do in the following.

The σ model has been discussed extensively in the literature, and here we only briefly outline its contents to define the quantities we need. The model contains an isotriplet of pseudoscalars, $\boldsymbol{\pi}$, and an isosinglet scalar, σ, grouped into

$$\Sigma = \sigma - i\boldsymbol{\tau}\cdot\boldsymbol{\pi}, \tag{5.2}$$

which transforms under global $\mathrm{SU}(2)_L\times\mathrm{SU}(2)_R$ as

$$\Sigma \to L\Sigma R^\dagger. \tag{5.3}$$

The nucleon wave function ψ has left and right components, $\psi_{L,R}=\frac{1}{2}(1\mp\gamma_5)\psi$, transforming as

$$\psi_L \to L\psi_L, \quad \psi_R \to R\psi_R. \tag{5.4}$$

The transformations can be made local by introducing the left and right gauge fields,

$$l_\mu \equiv \tfrac{1}{2}\boldsymbol{\tau}\cdot\mathbf{l}_\mu = \tfrac{1}{2}\boldsymbol{\tau}\cdot(\boldsymbol{\rho}_\mu-\mathbf{a}_\mu),$$
$$r_\mu \equiv \tfrac{1}{2}\boldsymbol{\tau}\cdot\mathbf{r}_\mu = \tfrac{1}{2}\boldsymbol{\tau}\cdot(\boldsymbol{\rho}_\mu+\mathbf{a}_\mu), \tag{5.5}$$

and their field strength tensors

$$l_{\mu\nu} = \partial_\mu l_\nu - \partial_\nu l_\mu + ig_V[l_\mu,l_\nu], \tag{5.6}$$

and similarly for $r_{\mu\nu}$. The vector and axial-vector mesons are given a mass by introducing a chiral-symmetry breaking mass term

$$\mathcal{L}_m = \tfrac{1}{2}m_\rho^2\mathrm{Tr}(l_\mu l^\mu + r_\mu r^\mu). \tag{5.7}$$

After the introduction of the gauge fields, the chiral symmetry can be restored by defining the following covariant derivatives for the nucleon and $(\sigma,\boldsymbol{\pi})$ fields,

$$\mathcal{D}_\mu\psi = (\partial_\mu + \tfrac{i}{2}g_V\boldsymbol{\tau}\cdot\boldsymbol{\rho}_\mu + \tfrac{i}{2}g_V\boldsymbol{\tau}\cdot\mathbf{a}_\mu\gamma_5)\psi,$$

$$\mathcal{D}_\mu\Sigma = \partial_\mu\Sigma + ig_V l_\mu\Sigma - ig_V\Sigma r_\mu. \tag{5.8}$$

A possible chiral-invariant Lagrangian is now given by

$$\begin{aligned}\mathcal{L}_0 = &\,\bar{\psi}i\gamma^\mu\mathcal{D}_\mu\psi - g_1(\bar{\psi}_L\Sigma\psi_R + \bar{\psi}_R\Sigma^\dagger\psi_L)\\&+g_2(\bar{\psi}_L\Sigma\Sigma^\dagger\Sigma\psi_R + \bar{\psi}_R\Sigma^\dagger\Sigma\Sigma^\dagger\psi_L)\\&+iC(\bar{\psi}_L\Sigma\gamma^\mu\mathcal{D}_\mu\Sigma^\dagger\psi_L + \bar{\psi}_R\Sigma^\dagger\gamma^\mu\mathcal{D}_\mu\Sigma\psi_R)\\&-\tfrac{1}{4}\mathrm{Tr}(l_{\mu\nu}l^{\mu\nu}+r_{\mu\nu}r^{\mu\nu}) + \tfrac{1}{4}\mathrm{Tr}(\mathcal{D}^\mu\Sigma^\dagger\mathcal{D}_\mu\Sigma)\\&-\tfrac{1}{4}\mu^2\mathrm{Tr}(\Sigma^\dagger\Sigma) - \tfrac{1}{8}\lambda^2\mathrm{Tr}(\Sigma^\dagger\Sigma)^2,\end{aligned} \tag{5.9}$$

where g_1, g_2, C, μ, and λ are free parameters.

The symmetry can be spontaneously broken by adding a term linear in the σ field,

$$\mathcal{L}_{SB} = f_\pi m_\pi^2\sigma, \tag{5.10}$$

with $f_\pi = 92.4$ MeV the pion decay constant. Choosing the ground state as $\langle\sigma\rangle = v$, this spontaneous symmetry breaking introduces a mixing between the $\boldsymbol{\pi}$ and $\mathbf{a}_\mu$ fields, which requires a redefinition of the fields, given by

$$\sigma \rightarrow \sigma + v,$$

$$\mathbf{a}_\mu \rightarrow \mathbf{A}_\mu - \frac{g_V v}{m_A^2} D_\mu \boldsymbol{\pi},$$

$$\boldsymbol{\pi} \rightarrow \frac{m_A}{m_\rho} \boldsymbol{\pi}, \tag{5.11}$$

where we defined $m_A^2 = m_\rho^2 + (g_V v)^2$, $v = (m_A/m_\rho)f_\pi$, and $D_\mu \boldsymbol{\pi} = \partial_\mu \boldsymbol{\pi} + g_V \boldsymbol{\pi} \times \boldsymbol{\rho}_\mu$. The shift of the σ field gives the nucleons a mass $M = (g_1 - g_2 v^2)v$, which imposes a constraint on g_1 and g_2.

Comparing the various pieces of the full Lagrangian $\mathcal{L}_0 + \mathcal{L}_m + \mathcal{L}_{SB}$ with the interaction Hamiltonians of Sec. II, we identify the following relations for the single-meson coupling constants:

$$g_{NN\sigma} = (g_1 - 3g_2 v^2) = M/v - 2g_2 v^2,$$

$$f_{NN\pi} = \frac{m_\pi}{2f_\pi} \left(2Cv^2 - \frac{m_\rho^2}{m_A^2} \right),$$

$$g_{NN\rho} = \tfrac{1}{2} g_V,$$

$$g_{NNA} = \frac{m_A}{m_\pi} \frac{\sqrt{m_A^2 - m_\rho^2}}{m_\rho} f_{NN\pi}. \tag{5.12}$$

The numerical value for C is obtained by imposing the Goldberger-Treiman [20] relation,

$$\frac{f_{NN\pi}}{m_\pi} = \frac{g_A}{2f_\pi}, \tag{5.13}$$

with $g_A = 1.2573$ the weak interaction axial-vector coupling constant. Similarly, the meson-pair coupling constants are found to be

$$g_{(\pi\pi)_0} = -\frac{m_\pi}{2f_\pi} \left(\frac{M}{f_\pi} - g_{NN\sigma} \frac{m_A}{m_\rho} \right),$$

$$g_{(\sigma\sigma)} = 3g_{(\pi\pi)_0} \frac{m_\rho^2}{m_A^2},$$

$$g_{(\pi\pi)_1} = \frac{m_\pi^2}{2f_\pi^2} \frac{m_\rho^2}{m_A^2} \left(g_A + \frac{m_\rho^2}{m_A^2} \right),$$

$$g_{(\pi\rho)_1} = \frac{g_{NN\rho}}{2f_\pi}(g_A + 1),$$

$$g_{(\pi\sigma)} = \frac{m_\pi^2}{2f_\pi^2} \frac{m_A^2 - 2m_\rho^2}{m_A m_\rho} \left(g_A + \frac{m_\rho^2}{m_A^2} \right). \tag{5.14}$$

Working out the various pieces of the Lagrangian we can also find relations for the meson-decay coupling constants. It is then found that the relation (5.1) is indeed satisfied, although in some cases the approximation is rather crude, as we already suspected. However, the meson-saturation assumption is still very useful to suggest the obvious relation

$$f_{(\pi\pi)_1} = g_{(\pi\pi)_1} (f_{NN\rho}/g_{NN\rho}). \tag{5.15}$$

VI. RESULTS AND DISCUSSION

The complete one-pair and two-pair potential can be written as

$$V(\alpha\beta) = V^{(1)}(\alpha\beta) + V^{(2)}(\alpha\beta) + V^{\mathrm{na}}(\alpha\beta) + V^{\mathrm{pv}}(\alpha\beta), \tag{6.1}$$

for the pairs $(\alpha\beta)$ discussed in this paper. To present the potentials in graphical form, we employ the meson-nucleon coupling constants and cutoff masses of a preliminary version of the Nijmegen extended soft-core (ESC) potential. The ESC potential is still under construction, but the present values for the coupling constants clearly suffice for illustrative purposes. The meson-nucleon coupling constants and cutoff masses are already listed in Table IV of the previous paper [1], while the pair coupling constants are here given in Table III. All pair coupling constants are fixed at their theoretical values as given in Sec. V. This constraint might be a bit too severe, but the values can at least be expected to be reasonable. Furthermore, in this way we can get a feeling about the importance of two-meson exchanges with respect to one-boson exchanges, because we do not introduce any new free parameters.

In Figs. 5 and 6, we compare the various types of one-pair and two-pair exchanges for $I = 0$ and $I = 1$, respectively. They consist of scalar 0^{++} exchanges $[(\pi\pi)_0$ and $(\sigma\sigma)]$, vector 1^{--} exchange $[(\pi\pi)_1]$, and axial 1^{++} exchanges $[(\pi\rho)_1$ and $(\pi\sigma)]$. The central $I = 0$ potential is clearly dominated by the one-pair $(\pi\pi)_1$ potential, whereas the scalar and vector two-pair potentials largely cancel each other. For $I = 1$, the scalar one-pair and two-pair potentials are the same, whereas the vector potentials change by a factor –3, resulting in a much smaller (but still attractive) central potential. For the spin-spin and tensor potentials the $I = 0$ and $I = 1$ cases differ by a simple factor of –3, where the two-pair axial tensor component turns out to be completely negligible.

In all cases, the $1/M$ corrections from the nonadiabatic expansion of the energy denominators and from the

pseudovector-vertex correction in the pion vertex function have the opposite sign. In the $(\pi\pi)_0$ potential the cancellation is even exact. The $1/M$ corrections to the spin-spin and tensor potentials are only due to the $(\pi\sigma)$ potential, whereas the $(\pi\pi)_0$ and $(\pi\pi)_1$ potentials only contribute to the central and spin-orbit potentials.

In Fig. 7 we compare the spin-orbit components from the one-pair potentials. They are all due to the $1/M$ nonadiabatic or pseudovector-vertex corrections in the $(\pi\pi)_0$ and $(\pi\pi)_1$ potentials. The $(\pi\pi)_1$ potential also has a spin-orbit potential due to the $1/M$ term in the $(\pi\pi)_1$ pair vertex (2.8b), as given in Eq. (C5) of Appendix C. This contribution is exactly the same as the nonadiabatic contribution, which means that in the $(\pi\pi)_1$ potential there is an even larger cancellation between the nonadiabatic (long-dashed line) and pseudovector-vertex (dash-dotted line) spin-orbit parts than Fig. 7 might suggest. Note that in the $(\pi\pi)_0$ potential the cancellation between the nonadiabatic (solid line) and pseudovector-vertex (short-dashed line) spin-orbit parts is exact, and so there is no spin-orbit potential from 0^{++} pair exchange. Obviously, if we were to take the pseudoscalar coupling $\bar\psi i\gamma_5\psi\phi$ for the pion, rather than the pseudovector coupling $\bar\psi\gamma_5\gamma_\mu\psi\partial^\mu\phi$ these cancellations do not occur, and we are left with the spin-orbit contribution from the nonadiabatic expansion.

Finally, we should mention that in some cases the two-pair diagrams are in principle included in the cases where we use the exchange of broad mesons. This is the case for the two-pair $(\pi\pi)_0$ and $(\pi\pi)_1$ potentials. Here we use in the Nijmegen work a broad ε and ρ one-boson-exchange potential. If such a broad meson exchange is included exactly, the two-pair $\pi\pi$ potentials should be omitted. When such broad mesons are included in a two-pole approximation [9, 10], however, a two-pair contribution might still be useful. Whether these two-pair contributions in that case should be included in full or partially suppressed is presently under investigation.

Let us now return to a comparison of this new ESC potential with the one-boson-exchange Nijm93 potential [15]. It is important to realize that both models contain essentially the same set of parameters, and so the ESC model is a true extension of the Nijm93 model. Using the linear σ model as a means to get a reasonable estimate for the various meson-pair coupling constants,

however, the contributions from the two-meson exchange diagrams (the planar and crossed-box diagrams as evaluated in the previous paper [1] as well as the one-pair and two-pair diagrams as evaluated in the present paper) are included without the introduction of any new parameters. The 14 free parameters of the ESC model are fitted to the 1993 Nijmegen representation of the χ^2 hypersurface of the NN scattering data below $T_{\rm lab} = 350$ MeV [21], updated with the inclusion of new data which have been published since then.

The results for the 10 energy bins are given in Table IV, where we compare the results from the updated partial-wave analysis with the Nijm93 and ESC potentials. Clearly, the inclusion of the two-meson exchanges in the ESC model allows for a substantially better description of the NN scattering data than what could be achieved with the one-boson-exchange Nijm93 model. At present, the ESC potential is the only meson-theoretical model which can give such a good description of the scattering data (using only a limited set of free parameters). The quality of the ESC potential is even better if we restrict its application to energies below $T_{\rm lab} \approx 300$ MeV, giving $\chi^2/N_{\rm data} = 1.137$ for the 0–290 MeV energy interval. This was to be expected, since the nonadiabatic expansion in principle is only valid below the pion-production threshold.

To summarize, the combined results of the present and the previous [1] paper show that it is possible to construct a nucleon-nucleon potential model, based on a chiral-symmetric Lagrangian, that gives a good description of the nucleon-nucleon scattering data. Fine-tuning of the 14 parameters of this extended model allows for a substantially better description of the data than what was possible with the 14-parameter one-boson-exchange Nijm93 model [15].

APPENDIX A: ENERGY INTEGRALS

We discuss here the treatment of the energy integrals that occur in the evaluation of the meson-pair potentials. To prevent displaying all the indices, we introduce the following convenient notations

$$\omega = \sqrt{\mathbf{k}^2 + m^2}, \quad \omega' = \sqrt{\mathbf{k}'^2 + m'^2},$$

$$A = E(\mathbf{p}) - \tfrac{1}{2}W, \quad A' = E(\mathbf{p}') - \tfrac{1}{2}W, \quad A'' = E(\mathbf{p}'') - \tfrac{1}{2}W, \tag{A1}$$

where $\mathbf{p}' - \mathbf{p} = \mathbf{k} + \mathbf{k}'$ and $\mathbf{p}'' = \mathbf{p} + \mathbf{k}$. Note that with this notation, $\mathbf{k}$ and $\mathbf{k}'$ correspond to $\mathbf{k}_1$ and $\mathbf{k}_2$, respectively, introduced in the main text.

(i) *The one-pair graph.* Here we encounter the integral

$$
\mathcal{J}_{1P}(\mathbf{p}', \mathbf{p}|W) = -(2\pi)^{-2}\,[W - 2E(\mathbf{p}')]\,[W - 2E(\mathbf{p})] \int dp_0' \int dp_0 \int dk_0' \int dk_0 \; \delta^4(p' - p - k - k')
$$
$$
\times [k'^2 - m'^2 + i\delta]^{-1}\,[F_W^{(a)}(\mathbf{p}', p_0')F_W^{(b)}(-\mathbf{p}', -p_0')]^{-1}[F_W^{(b)}(-\mathbf{p} - \mathbf{k}, -p_0 - k_0)]^{-1}
$$
$$
\times [k^2 - m^2 + i\delta]^{-1}\,[F_W^{(a)}(\mathbf{p}, p_0)F_W^{(b)}(-\mathbf{p}, -p_0)]^{-1}. \tag{A2}
$$

Similar integrals were treated in [16], to which we refer for the method of evaluation. We first bring the integral into the form

$$
\mathcal{J}_{1P} = (2\pi)^{-4}[4A'A] \int_{-\infty}^{+\infty} d\alpha \int_{-\infty}^{+\infty} d\beta \int_{-\infty}^{+\infty} dp_0' \int_{-\infty}^{+\infty} dp_0 \int_{-\infty}^{+\infty} dk_0' \int_{-\infty}^{+\infty} dk_0 \int_{-\infty}^{+\infty} dp_0''\; e^{i\alpha(p_0' - k_0' - p_0'')}e^{i\beta(p_0'' - p_0 - k_0)}
$$
$$
\times [\omega'^2 - k_0'^2 - i\delta]^{-1}[\omega^2 - k_0^2 - i\delta]^{-1}[A'^2 - p_0'^2 - i\delta]^{-1}[A'' + p_0'' - i\delta]^{-1}[A^2 - p_0^2 - i\delta]^{-1}. \tag{A3}
$$

The energy-variable integrations can be performed in a straightforward manner using the residue theorem, e.g.,

$$
\int_{-\infty}^{+\infty} dk_0\; \frac{e^{i\beta k_0}}{\omega^2 - k_0^2 - i\delta} = \frac{2\pi i}{2\omega}e^{\mp i\beta\omega}, \tag{A4}
$$

where in the exponential the $(-)$-sign and the $(+)$-sign apply to $\beta > 0$ and $\beta < 0$, respectively. Also,

$$
\int_{-\infty}^{+\infty} dp_0''\; \frac{e^{i\beta p_0''}}{A'' + p_0'' - i\delta} = \begin{cases} 2\pi i\; e^{-i\beta A''}, & \beta > 0, \\ 0, & \beta < 0. \end{cases} \tag{A5}
$$

Keeping track of the signs in the exponentials, the intermediate result is

$$
\mathcal{J}_{1P} = (2\pi)^{-4}(2\pi i)^5[4\omega\omega']^{-1} \left\{ \int_0^\infty d\alpha \int_\alpha^\infty d\beta\; e^{-i\alpha(\omega' + A' - A'')}e^{-i\beta(\omega + A + A'')} \right.
$$
$$
+ \int_{-\infty}^0 d\alpha \int_0^\infty d\beta\; e^{+i\alpha(\omega' + A' + A'')}e^{-i\beta(\omega + A + A'')}
$$
$$
\left. + \int_{-\infty}^0 d\alpha \int_\alpha^0 d\beta\; e^{+i\alpha(\omega' + A' + A'')}e^{+i\beta(\omega + A - A'')} \right\}. \tag{A6}
$$

Performing the remaining elementary integrals, we end up with

$$
\mathcal{J}_{1P} = -\frac{2\pi i}{4\omega\omega'} \left\{ \frac{1}{A' + A'' + \omega'}\,\frac{1}{A + A' + \omega + \omega'} + \frac{1}{A' + A'' + \omega'}\,\frac{1}{A + A'' + \omega} + \frac{1}{A + A'' + \omega}\,\frac{1}{A + A' + \omega + \omega'} \right\}. \tag{A7}
$$

The terms in the curly brackets correspond to the different time-ordered graphs (a), (b), and (c) of Fig. 3.

(ii) *The two-pair graph.* Here the integral to be performed is

$$
\mathcal{J}_{2P}(\mathbf{p}', \mathbf{p}|W) = -(2\pi)^{-2}\,[W - 2E(\mathbf{p}')]\,[W - 2E(\mathbf{p})] \int dp_0' \int dp_0 \int dk_0' \int dk_0\; \delta^4(p' - p - k - k')[k'^2 - m'^2 + i\delta]^{-1}
$$
$$
\times [F_W^{(a)}(\mathbf{p}', p_0')F_W^{(b)}(-\mathbf{p}', -p_0')]^{-1}[k^2 - m^2 + i\delta]^{-1}\,[F_W^{(a)}(\mathbf{p}, p_0)\,F_W^{(b)}(-\mathbf{p}, -p_0)]^{-1}. \tag{A8}
$$

This integral can be brought into the form

$$
\mathcal{J}_{2P} = -(2\pi)^{-3}[4A'A] \int_{-\infty}^{+\infty} d\alpha \int_{-\infty}^{+\infty} dp_0' \int_{-\infty}^{+\infty} dp_0 \int_{-\infty}^{+\infty} dk_0' \int_{-\infty}^{+\infty} dk_0\; e^{i\alpha(p_0' - p_0 - k_0 - k_0')}
$$
$$
\times [\omega'^2 - k_0'^2 - i\delta]^{-1}[\omega^2 - k_0^2 - i\delta]^{-1}[A'^2 - p_0'^2 - i\delta]^{-1}[A^2 - p_0^2 - i\delta]^{-1}. \tag{A9}
$$

The evaluation of the energy-variable integrals gives in this case

9

$$\mathcal{J}_{2P} = -(2\pi)^{-3}(2\pi i)^4 \left[4\omega\omega'\right]^{-1} \left\{ \int_0^\infty d\alpha \; e^{-i\alpha(\omega+\omega'+A+A')} + \int_{-\infty}^0 d\alpha \; e^{+i\alpha(\omega+\omega'+A+A')} \right\}. \tag{A10}$$

The two terms correspond to the time-ordered graph (d) of Fig. 3 and its "mirror" graph. Carrying out the final α integrations leads to the final expression

$$\mathcal{J}_{2P} = \frac{2\pi i}{4\omega\omega'} \frac{2}{A + A' + \omega + \omega'}. \tag{A11}$$

APPENDIX B: ISOSPIN FACTORS

In this Appendix we review the calculation of the isospin factors. The isospin factor comes from the evaluation of all possible contractions for the vacuum matrix element of the product of the meson fields coming from the contractions of the interaction Hamiltonians at the different vertices. For the one-pair diagrams we label the NNm_1m_2 vertex with (1), the meson vertex on the other nucleon line with (2), and the pion vertex with (3). The pion is propagating with momentum $\mathbf{k}_1$ and the other meson with momentum $\mathbf{k}_2$. The isospin factors are then found to be

$$
\begin{aligned}
(\pi\pi)_0 : \; & \langle 0| \boldsymbol{\pi}\cdot\boldsymbol{\pi}(1)\boldsymbol{\tau}_2\cdot\boldsymbol{\pi}(2)\boldsymbol{\tau}_2\cdot\boldsymbol{\pi}(3)|0\rangle = (\delta_{im}\delta_{in} + \delta_{in}\delta_{im})\tau_{2m}\tau_{2n} = 6, \\
(\sigma\sigma) : \; & \langle 0|\sigma\sigma(1)\sigma(2)\sigma(3)|0\rangle = (12, 13 + 13, 12)_{\text{contractions}} = 2, \\
(\pi\pi)_1 : \; & \langle 0|\boldsymbol{\tau}_1\cdot\boldsymbol{\pi} \times \partial^\mu\boldsymbol{\pi}(1)\boldsymbol{\tau}_2\cdot\boldsymbol{\pi}(2)\boldsymbol{\tau}_2\cdot\boldsymbol{\pi}(3)|0\rangle = \varepsilon_{ijk}\tau_{1k}\tau_{2m}\tau_{2n}\langle 0|\pi_i(1)\partial^\mu\pi_j(1)\pi_m(2)\pi_n(3)|0\rangle \\
& \qquad\qquad = \varepsilon_{ijk}\tau_{1k}\tau_{2m}\tau_{2n}[\delta_{im}\delta_{jn}\partial^\mu(3) + \delta_{in}\delta_{jm}\partial^\mu(2)] \\
& \qquad\qquad = 2i\boldsymbol{\tau}_1\cdot\boldsymbol{\tau}_2(\partial_1^\mu - \partial_2^\mu), \\
(\pi\rho)_1 : \; & \langle 0|\boldsymbol{\tau}_1\cdot\boldsymbol{\pi} \times \boldsymbol{\rho}(1)\boldsymbol{\tau}_2\cdot\boldsymbol{\rho}(2)\boldsymbol{\tau}_2\cdot\boldsymbol{\pi}(3)|0\rangle = \varepsilon_{ijk}\tau_{1k}\tau_{2m}\tau_{2n}\delta_{in}\delta_{jm} = -2i\boldsymbol{\tau}_1\cdot\boldsymbol{\tau}_2, \\
(\pi\sigma) : \; & \langle 0|\boldsymbol{\tau}_1\cdot\boldsymbol{\pi}(1)\sigma(1)\sigma(2)\boldsymbol{\tau}_2\cdot\boldsymbol{\pi}(3)|0\rangle = \tau_{1i}\delta_{im}\tau_{2m} = \boldsymbol{\tau}_1\cdot\boldsymbol{\tau}_2.
\end{aligned}
$$

For the two-pair diagrams, we label the NNm_1m_2 vertices on each nucleon line by (1) and (2), respectively. We then find

$$
\begin{aligned}
(\pi\pi)_0 : \; & \langle 0|\boldsymbol{\pi}\cdot\boldsymbol{\pi}(1)\boldsymbol{\pi}\cdot\boldsymbol{\pi}(2)|0\rangle = (\delta_{im}\delta_{im} + \delta_{im}\delta_{im}) = 6, \\
(\sigma\sigma) : \; & \langle 0|\sigma\sigma(1)\sigma\sigma(2)|0\rangle = 2, \\
(\pi\pi)_1 : \; & \langle 0|\boldsymbol{\tau}_1\cdot\boldsymbol{\pi} \times \partial^\mu\boldsymbol{\pi}(1)\boldsymbol{\tau}_2\cdot\boldsymbol{\pi} \times \partial^\nu\boldsymbol{\pi}(2)|0\rangle = \varepsilon_{ijk}\varepsilon_{mnl}\tau_{1k}\tau_{2l}\langle 0|\pi_i(1)\partial^\mu\pi_j(1)\pi_m(2)\partial^\nu\pi_n(2)|0\rangle \\
& \qquad\qquad = 2\boldsymbol{\tau}_1\cdot\boldsymbol{\tau}_2(\partial_2^\mu\partial_2^\nu - \partial_1^\mu\partial_2^\nu) \\
& \qquad\qquad = \boldsymbol{\tau}_1\cdot\boldsymbol{\tau}_2(\partial_1^\mu - \partial_2^\mu)(\partial_1^\nu - \partial_2^\nu), \\
(\pi\rho)_1 : \; & \langle 0|\boldsymbol{\tau}_1\cdot\boldsymbol{\pi} \times \boldsymbol{\rho}(1)\boldsymbol{\tau}_2\cdot\boldsymbol{\pi} \times \boldsymbol{\rho}(2)|0\rangle = \varepsilon_{ijk}\varepsilon_{mnl}\tau_{1k}\tau_{2l}\delta_{im}\delta_{jn} = 2\boldsymbol{\tau}_1\cdot\boldsymbol{\tau}_2, \\
(\pi\sigma) : \; & \langle 0|\boldsymbol{\tau}_1\cdot\boldsymbol{\pi}(1)\sigma(1)\boldsymbol{\tau}_2\cdot\boldsymbol{\pi}(2)\sigma(2)|0\rangle = \tau_{1i}\delta_{im}\tau_{2m} = \boldsymbol{\tau}_1\cdot\boldsymbol{\tau}_2.
\end{aligned}
$$

We should point out that for the $(\pi\pi)_1$ vertices the isospin factors are defined to be $2i\boldsymbol{\tau}_1\cdot\boldsymbol{\tau}_2$ and $\boldsymbol{\tau}_1\cdot\boldsymbol{\tau}_2$ for the one-pair and two-pair potentials, respectively, because the ∂_i^μ dependence, i.e., the $\mathbf{k}_i$ dependence, is already included in the operators $O_{\alpha\beta,p}^{(n)}$ given in Tables I and II.

APPENDIX C: COORDINATE-SPACE POTENTIALS

The explicit formulas for the soft-core meson-pair potentials are given below.
(i) Scalar $\pi \otimes \pi$ ($I = 0$) pairs:

$$V_{\text{pair}}^{(1)}(r) = 6\frac{g_{(\pi\pi)_0}}{m_\pi}\frac{f_{NN\pi}^2}{m_\pi^2}\left[I'_{2,\pi}(r)\right]^2, \tag{C1}$$

$$V_{\text{pair}}^{(2)}(r) = -3\frac{g_{(\pi\pi)_0}^2}{m_\pi^2}\frac{2}{\pi}\int_0^\infty d\lambda \left[F_\pi(\lambda, r)\right]^2. \tag{C2}$$

(ii) Scalar $\sigma \otimes \sigma$ pairs:

10

$$V_{\text{pair}}^{(1)}(r) = 2\frac{g_{(\sigma\sigma)}}{m_\pi} g_{NN\sigma}^2 \left[I_{2,\sigma}(r)\right]^2, \tag{C3}$$

$$V_{\text{pair}}^{(2)}(r) = -\frac{g_{(\sigma\sigma)}^2}{m_\pi^2} \frac{2}{\pi} \int_0^\infty d\lambda \left[F_\sigma(\lambda, r)\right]^2. \tag{C4}$$

(iii) Vector $\pi \otimes \pi$ $(I = 1)$ pairs:

$$V_{\text{pair}}^{(1)}(r) = 4\left(\boldsymbol{\tau}_1 \cdot \boldsymbol{\tau}_2\right) \frac{g_{(\pi\pi)_1}}{m_\pi^2} \frac{f_{NN\pi}^2}{m_\pi^2} \left\{ \frac{2}{\pi} \int_0^\infty d\lambda \left[F_\pi'(\lambda, r)\right]^2 - \frac{1}{M} \frac{1}{r^2} [I_{2,\pi}'(r)]^2 \, \mathbf{L} \cdot \mathbf{S} \right.$$

$$\left. - \frac{1 + \kappa_1}{3M} \left[\frac{1}{r} I_{2,\pi}' \left(\frac{1}{r} I_{2,\pi}' + 2 I_{2,\pi}''\right)(r) \left(\boldsymbol{\sigma}_1 \cdot \boldsymbol{\sigma}_2\right) + \frac{1}{r} I_{2,\pi}' \left(\frac{1}{r} I_{2,\pi}' - I_{2,\pi}''\right)(r) \, S_{12} \right] \right\}, \tag{C5}$$

$$V_{\text{pair}}^{(2)}(r) = -\left(\boldsymbol{\tau}_1 \cdot \boldsymbol{\tau}_2\right) \frac{g_{(\pi\pi)_1}^2}{m_\pi^4} \frac{2}{\pi} \int_0^\infty d\lambda \, F_\pi(\lambda, r) \left[\frac{\Lambda_\pi^3}{8\pi\sqrt{\pi}} \, e^{-\frac{1}{4}\Lambda_\pi^2 r^2} - 2\lambda^2 F_\pi(\lambda, r) \right]. \tag{C6}$$

(iv) Axial $\pi \otimes \rho$ $(I = 1)$ pairs:

$$V_{\text{pair}}^{(1)}(r) = -\tfrac{2}{3}\left(\boldsymbol{\tau}_1 \cdot \boldsymbol{\tau}_2\right) \frac{g_{(\pi\rho)_1}}{m_\pi} \frac{f_{NN\pi}}{m_\pi} \frac{g_{NN\rho}}{M_N} \left\{ (1 + \kappa_\rho) \, I_{2,\pi}' I_{2,\rho}'(r) \left[S_{12} - 2(\boldsymbol{\sigma}_1 \cdot \boldsymbol{\sigma}_2)\right] \right.$$

$$\left. + \left(I_{2,\pi}'' + \frac{2}{r} I_{2,\pi}'\right) I_{2,\rho}(r) \left(\boldsymbol{\sigma}_1 \cdot \boldsymbol{\sigma}_2\right) + \left(I_{2,\pi}'' - \frac{1}{r} I_{2,\pi}'\right) I_{2,\rho}(r) \, S_{12} \right\}, \tag{C7}$$

$$V_{\text{pair}}^{(2)}(r) = -\left(\boldsymbol{\tau}_1 \cdot \boldsymbol{\tau}_2\right)(\boldsymbol{\sigma}_1 \cdot \boldsymbol{\sigma}_2) \frac{g_{(\pi\rho)_1}^2}{m_\pi^2} \frac{2}{\pi} \int_0^\infty d\lambda \, F_\pi F_\rho(\lambda, r). \tag{C8}$$

(v) Pseudovector $\pi \otimes \sigma$ pairs:

$$V_{\text{pair}}^{(1)}(r) = \tfrac{2}{3}\left(\boldsymbol{\tau}_1 \cdot \boldsymbol{\tau}_2\right) g_{NN\sigma} \frac{g_{(\pi\sigma)}}{m_\pi^2} \frac{f_{NN\pi}}{m_\pi} \left\{ \left[\left(I_{2,\pi}'' + \frac{2}{r} I_{2,\pi}'\right) I_{2,\sigma} - I_{2,\pi}' I_{2,\sigma}' \right](r) \left(\boldsymbol{\sigma}_1 \cdot \boldsymbol{\sigma}_2\right) \right.$$

$$\left. + \left[\left(I_{2,\pi}'' - \frac{1}{r} I_{2,\pi}'\right) I_{2,\sigma} - I_{2,\pi}' I_{2,\sigma}' \right](r) \, S_{12} \right\}, \tag{C9}$$

$$V_{\text{pair}}^{(2)}(r) = \tfrac{1}{6}\left(\boldsymbol{\tau}_1 \cdot \boldsymbol{\tau}_2\right) \frac{g_{(\pi\sigma)}^2}{m_\pi^4} \frac{2}{\pi} \int_0^\infty d\lambda \left\{ \left[\left(F_\pi'' + \frac{2}{r} F_\pi'\right) F_\sigma + \left(F_\sigma'' + \frac{2}{r} F_\sigma'\right) F_\pi - 2F_\pi' F_\sigma' \right](\lambda, r) \left(\boldsymbol{\sigma}_1 \cdot \boldsymbol{\sigma}_2\right) \right.$$

$$\left. + \left[\left(F_\pi'' - \frac{1}{r} F_\pi'\right) F_\sigma + \left(F_\sigma'' - \frac{1}{r} F_\sigma'\right) F_\pi - 2F_\pi' F_\sigma' \right](\lambda, r) \, S_{12} \right\}. \tag{C10}$$

[1] Th.A. Rijken and V.G.J. Stoks, Phys. Rev. C **54**, 2851 (1996), the preceding paper.

[2] M.M. Nagels, Th.A. Rijken, and J.J. de Swart, Phys. Rev. D **17**, 768 (1978).

[3] R. Dolen, D. Horn, and C. Schmid, Phys. Rev. **166**, 1768 (1968); H. Harari, Phys. Rev. Lett. **20**, 1395 (1968); F.J. Gilman, H. Harari, and Y. Zarmi, *ibid.* **21**, 323 (1968).

[4] J.J. de Swart, Th.A. Rijken, P.M. Maessen, and R.G. Timmermans, Nuovo Cimento A **102**, 203 (1989).

[5] S. Weinberg, Phys. Lett. B **251**, 288 (1990); Nucl. Phys. **B363**, 3 (1991); C. Ordóñez and U. van Kolck, Phys. Lett. B **291**, 459 (1992).

[6] J. Schwinger, Phys. Rev. **167**, 1432 (1968).

[7] S. Weinberg, Phys. Rev. **166**, 1568 (1968); **177**, 2604 (1969).

[8] Although the existence of the scalar nonet is still controversial, there appears to be evidence for a scalar–isoscalar resonant state $0^{++}(750)$; see M. Svec, A. de Lesquen, and L. van Rossum, Phys. Rev. D **46**, 949 (1992) and M. Svec, *ibid.* **53**, 2343 (1996).

[9] J. Schwinger, Phys. Rev. D **3**, 1967 (1971).

[10] J. Binstock and R.A. Bryan, Phys. Rev. D **4**, 1341 (1971).

[11] J.J. de Swart and M. M. Nagels, Fortschr. Phys. **28**, 215 (1978).

[12] A. Manohar and H. Georgi, Nucl. Phys. **B234**, 189 (1984); S. Weinberg, Physica (Amsterdam) **96A**, 327 (1979).

[13] E. Witten, Nucl. Phys. **B160**, 57 (1979).

[14] M. Gell-Mann and M. Lévy, Nuovo Cimento **16**, 705 (1960).

[15] V.G.J. Stoks, R.A.M. Klomp, C.P.F. Terheggen, and J.J. de Swart, Phys. Rev. C **49**, 2950 (1994).

[16] Th.A. Rijken, Ann. Phys. (N.Y.) **208**, 253 (1991).

[17] S. Gasiorowicz and D.A. Geffen, Rev. Mod. Phys. **41**, 531 (1969).

[18] B.W. Lee, *Chiral Dynamics* (Gordon and Breach, New York, 1972).

[19] P. Ko and S. Rudaz, Phys. Rev. D **50**, 6877 (1994).

[20] M.L. Goldberger and S.B. Treiman, Phys. Rev. **110**, 1178 (1958).

[21] V.G.J. Stoks, R.A.M. Klomp, M.C.M. Rentmeester, and J.J. de Swart, Phys. Rev. C **48**, 792 (1993).

TABLE I. The one-pair isospin factors $C^{(1)}(\alpha\beta)$ and momentum operators $O^{(1)}_{\alpha\beta,p}(\mathbf{k}_1,\omega_1;\mathbf{k}_2,\omega_2)$. The index p labels the three time-ordered contributions of Fig. 3 and is only of relevance for the $(\pi\pi)_1$ entry, where they are shown as a row vector. Note that $\kappa_1 = (f/g)_{(\pi\pi)_1}$.

$(\alpha\beta)$	$C^{(1)}(\alpha\beta)$	$O^{(1)}_{\alpha\beta,p}(\mathbf{k}_1,\omega_1;\mathbf{k}_2,\omega_2)$
$(\pi\pi)_0$	6	$-\mathbf{k}_1\cdot\mathbf{k}_2 + \frac{i}{2}(\boldsymbol{\sigma}_1+\boldsymbol{\sigma}_2)\cdot(\mathbf{k}_1\times\mathbf{k}_2)$
$(\sigma\sigma)$	2	1
$(\pi\pi)_1$	$2i\boldsymbol{\tau}_1\cdot\boldsymbol{\tau}_2$	$i\left[\mathbf{k}_1\cdot\mathbf{k}_2 - \frac{i}{2}(\boldsymbol{\sigma}_1+\boldsymbol{\sigma}_2)\cdot(\mathbf{k}_1\times\mathbf{k}_2)\right](\omega_1-\omega_2;\ -\omega_1-\omega_2;\ -\omega_1+\omega_2)$
		$+\frac{i}{M}\left[(1+\kappa_1)\boldsymbol{\sigma}_1\cdot(\mathbf{k}_1\times\mathbf{k}_2)\boldsymbol{\sigma}_2\cdot(\mathbf{k}_1\times\mathbf{k}_2) + \frac{i}{2}(\boldsymbol{\sigma}_1+\boldsymbol{\sigma}_2)\cdot(\mathbf{k}_1\times\mathbf{k}_2)\,\mathbf{q}\cdot(\mathbf{k}_1-\mathbf{k}_2)\right]$
$(\pi\rho)_1$	$-2i\boldsymbol{\tau}_1\cdot\boldsymbol{\tau}_2$	$\frac{i}{M}\left[\boldsymbol{\sigma}_1\cdot\mathbf{k}_1\boldsymbol{\sigma}_2\cdot\mathbf{k}_1 + \frac{1}{2}(1+\kappa_\rho)(\boldsymbol{\sigma}_1\cdot\mathbf{k}_1\boldsymbol{\sigma}_2\cdot\mathbf{k}_2 + \boldsymbol{\sigma}_1\cdot\mathbf{k}_2\boldsymbol{\sigma}_2\cdot\mathbf{k}_1 - 2\boldsymbol{\sigma}_1\cdot\boldsymbol{\sigma}_2\mathbf{k}_1\cdot\mathbf{k}_2)\right]$
$(\pi\sigma)$	$\boldsymbol{\tau}_1\cdot\boldsymbol{\tau}_2$	$\left[\boldsymbol{\sigma}_1\cdot\mathbf{k}_1\boldsymbol{\sigma}_2\cdot\mathbf{k}_2 + \boldsymbol{\sigma}_1\cdot\mathbf{k}_2\boldsymbol{\sigma}_2\cdot\mathbf{k}_1 - 2\boldsymbol{\sigma}_1\cdot\mathbf{k}_1\boldsymbol{\sigma}_2\cdot\mathbf{k}_1\right]$

TABLE II. The two-pair isospin factors $C^{(2)}(\alpha\beta)$ and momentum operators $O^{(2)}_{\alpha\beta,p}(\mathbf{k}_1,\omega_1;\mathbf{k}_2,\omega_2)$. The index p labels the two time-ordered contributions of Fig. 3 but is of no relevance in the final result.

$(\alpha\beta)$	$C^{(2)}(\alpha\beta)$	$O^{(2)}_{\alpha\beta,p}(\mathbf{k}_1,\omega_1;\mathbf{k}_2,\omega_2)$
$(\pi\pi)_0$	6	1
$(\sigma\sigma)$	2	1
$(\pi\pi)_1$	$\boldsymbol{\tau}_1\cdot\boldsymbol{\tau}_2$	$(\omega_1-\omega_2)^2$
$(\pi\rho)_1$	$2\boldsymbol{\tau}_1\cdot\boldsymbol{\tau}_2$	$\boldsymbol{\sigma}_1\cdot\boldsymbol{\sigma}_2$
$(\pi\sigma)$	$\boldsymbol{\tau}_1\cdot\boldsymbol{\tau}_2$	$\boldsymbol{\sigma}_1\cdot(\mathbf{k}_1-\mathbf{k}_2)\boldsymbol{\sigma}_2\cdot(\mathbf{k}_1-\mathbf{k}_2)$

TABLE III. Pair-meson coupling constants employed in the potentials shown in Figs. 5–7. Coupling constants are at $\mathbf{k}^2 = 0$. All coupling constants are fixed at their theoretical values as derived in Sec. V.

J^{PC}	$(\alpha\beta)$	$g/4\pi$	$f/4\pi$
0^{++}	$(\pi\pi)_0$	-0.412	
0^{++}	$(\sigma\sigma)$	-0.482	
1^{--}	$(\pi\pi)_1$	0.058	0.216
1^{++}	$(\pi\rho)_1$	0.598	
1^{++}	$(\pi\sigma)$	0.053	

TABLE IV. χ^2 and χ^2 per datum ($\chi^2_{\mathrm{p.d.p.}}$) at the ten energy bins for the updated partial-wave analysis (PWA) and the ESC and Nijm93 potential models. N_{data} lists the number of data within each energy bin. The bottom line gives the results for the total 0–350 MeV interval.

Bin(MeV)	N_{data}	PWA		ESC		Nijm93	
		χ^2	$\chi^2_{\mathrm{p.d.p.}}$	χ^2	$\chi^2_{\mathrm{p.d.p.}}$	χ^2	$\chi^2_{\mathrm{p.d.p.}}$
0.0–0.5	145	144.45	0.996	146.15	1.008	185.78	1.28
0.5–2	68	42.97	0.632	47.38	0.697	55.06	0.81
2–8	110	106.28	0.966	115.19	1.047	128.92	1.17
8–17	296	276.31	0.933	326.31	1.102	368.20	1.24
17–35	359	279.54	0.829	332.10	0.925	393.92	1.10
35–75	585	567.18	0.970	697.19	1.192	1337.28	2.29
75–125	399	409.58	1.027	421.89	1.057	480.96	1.20
125–183	760	820.69	1.080	936.53	1.232	1443.10	1.90
183–290	1047	1035.48	0.989	1261.50	1.205	1995.71	1.91
290–350	992	997.02	1.005	1706.75	1.721	2866.39	2.89
0–350	4761	4697.50	0.987	5990.99	1.258	9255.32	1.94
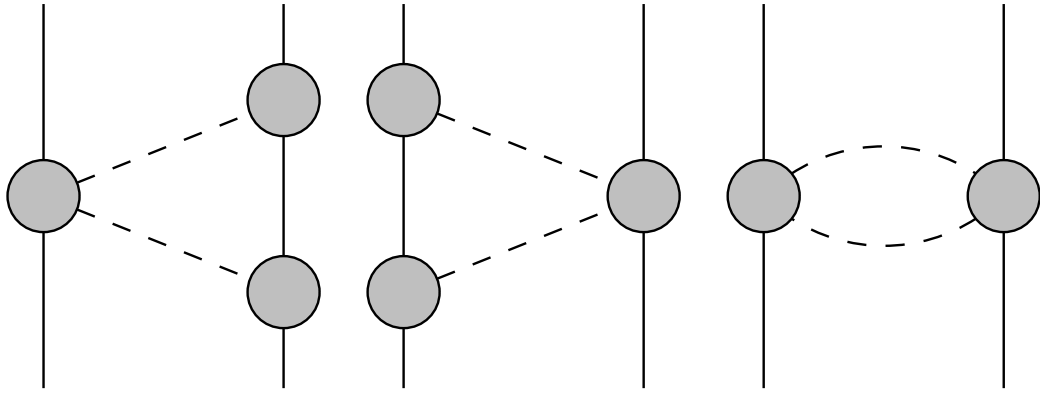
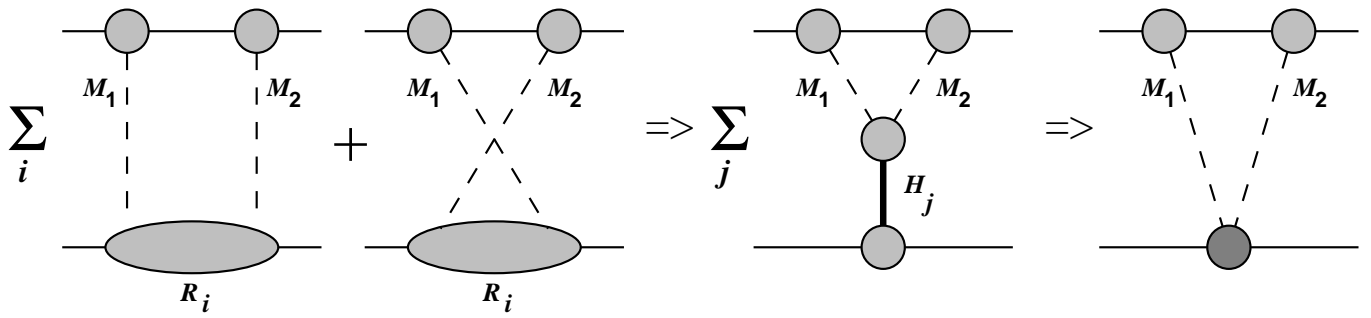FIG. 1. Feynman one-pair and two-pair diagrams.

FIG. 2. "Duality" picture of the meson-pair potentials. R_i represents a nucleon resonance, H_j the intermediating heavy boson, and M_1 and M_2 are the mesons being exchanged.
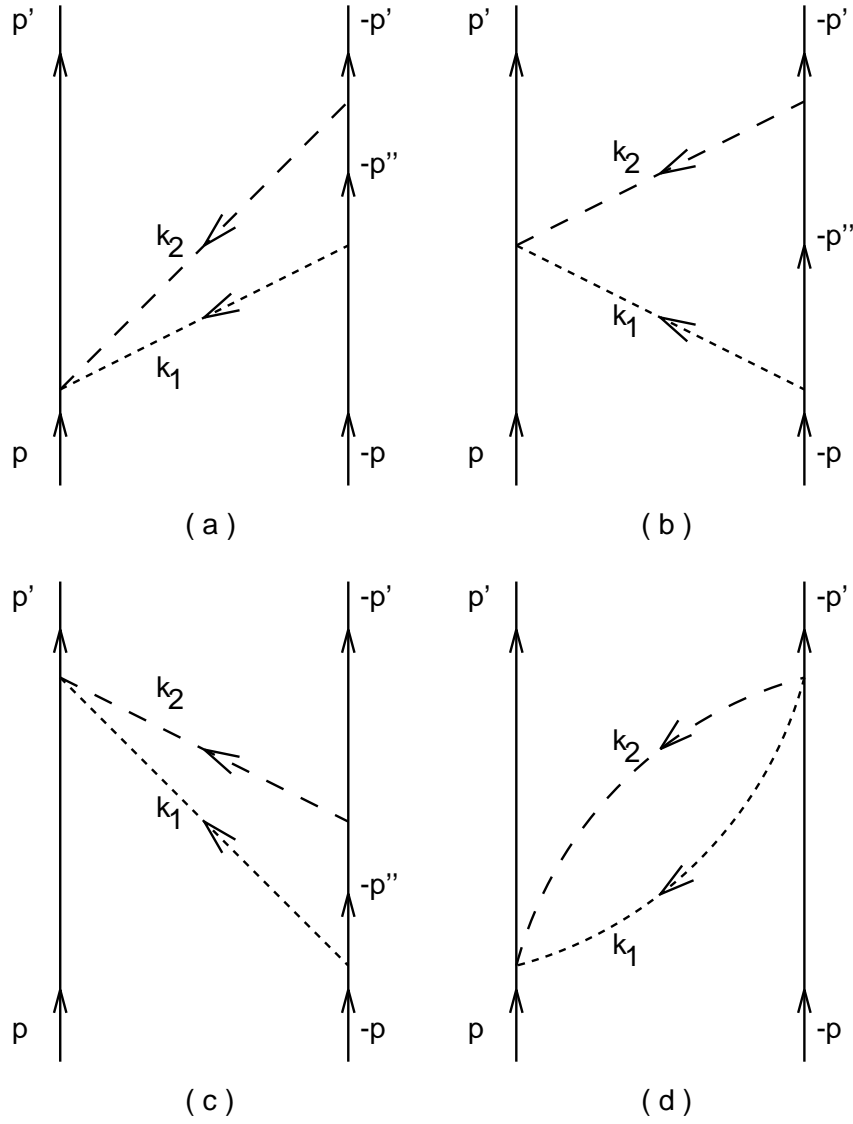
FIG. 3. Time-ordered (a–c) one-pair and (d) two-pair diagrams. The dotted line with momentum $\mathbf{k}_1$ refers to the pion and the dashed line with momentum $\mathbf{k}_2$ refers to one of the other (vector, scalar, or pseudoscalar) mesons. To these we have to add the "mirror" diagrams, where for the one-pair diagrams the pair vertex occurs on the other nucleon line.
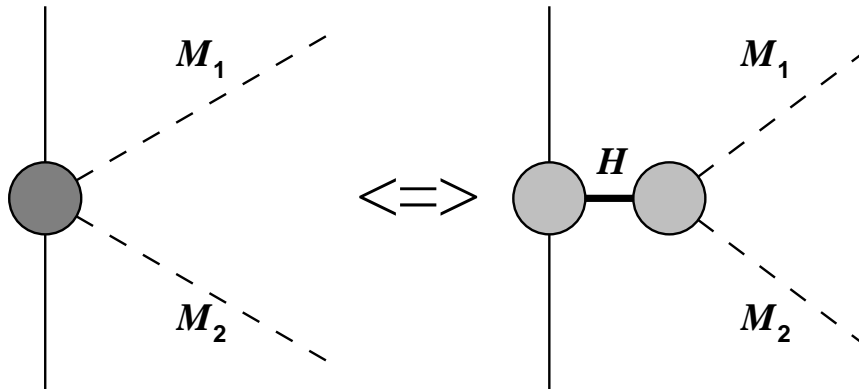
FIG. 4. Meson saturation of a pair vertex. The mesons are denoted by M_1 and M_2, and the intermediating heavy boson by H.
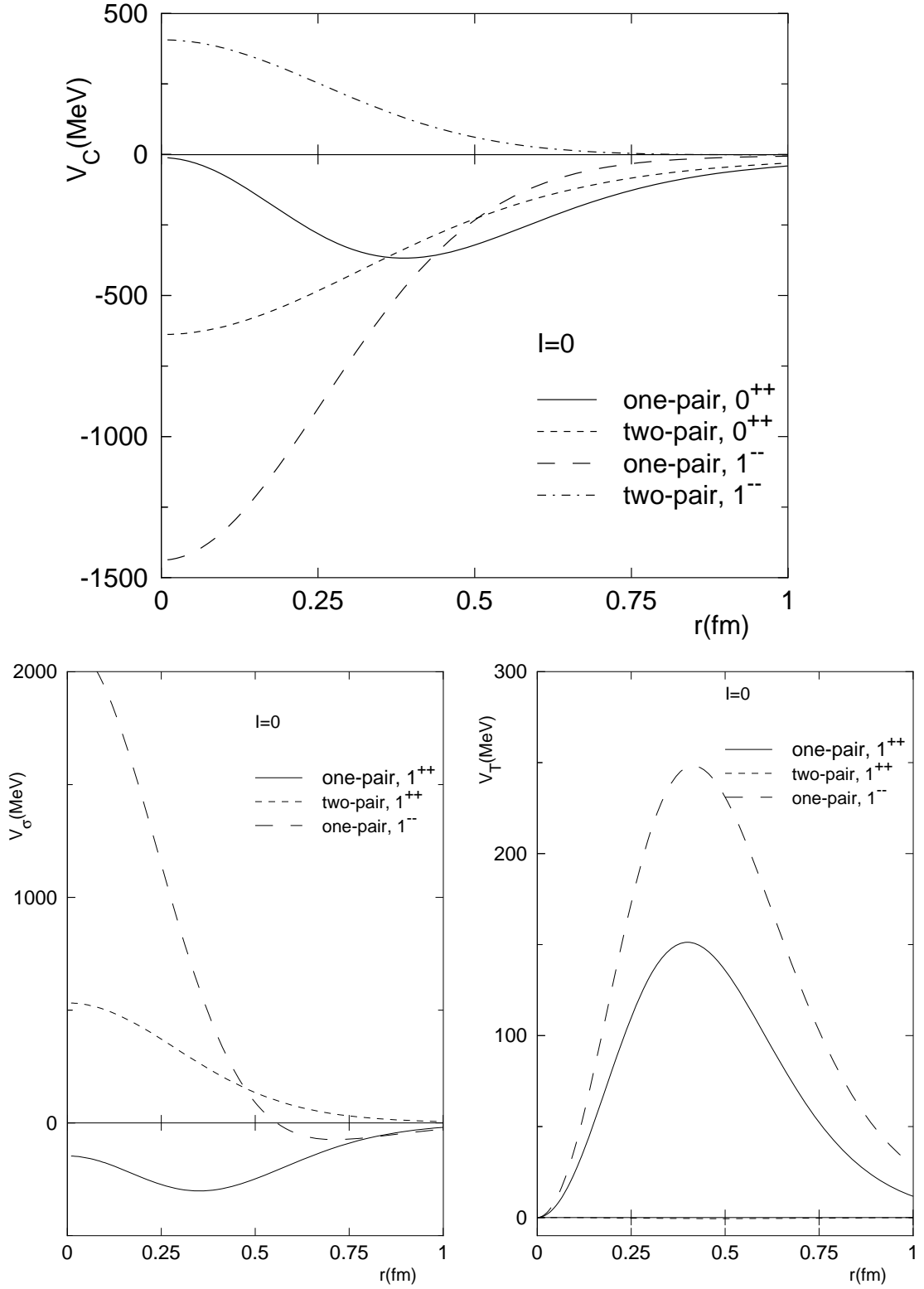
FIG. 5. Central, spin-spin, and tensor components of the $I = 0$ one-pair and two-pair potentials for (a) $r \leq 1$ fm and (b) $1 \leq r \leq 2$ fm. The pairs considered are 0^{++}: $(\pi\pi)_0$ and $(\sigma\sigma)$; 1^{--}: $(\pi\pi)_1$; and 1^{++}: $(\pi\rho)_1$ and $(\pi\sigma)$.
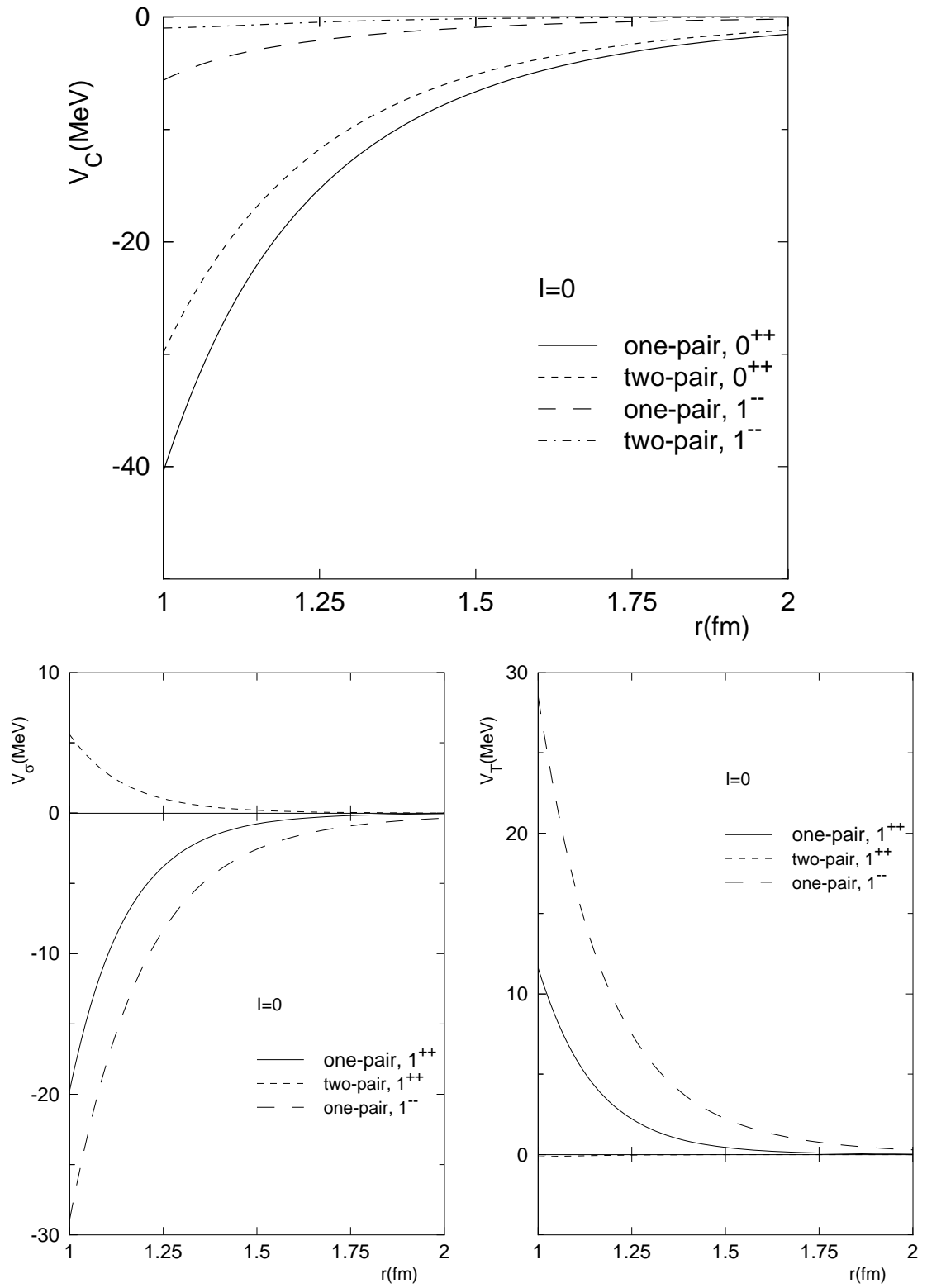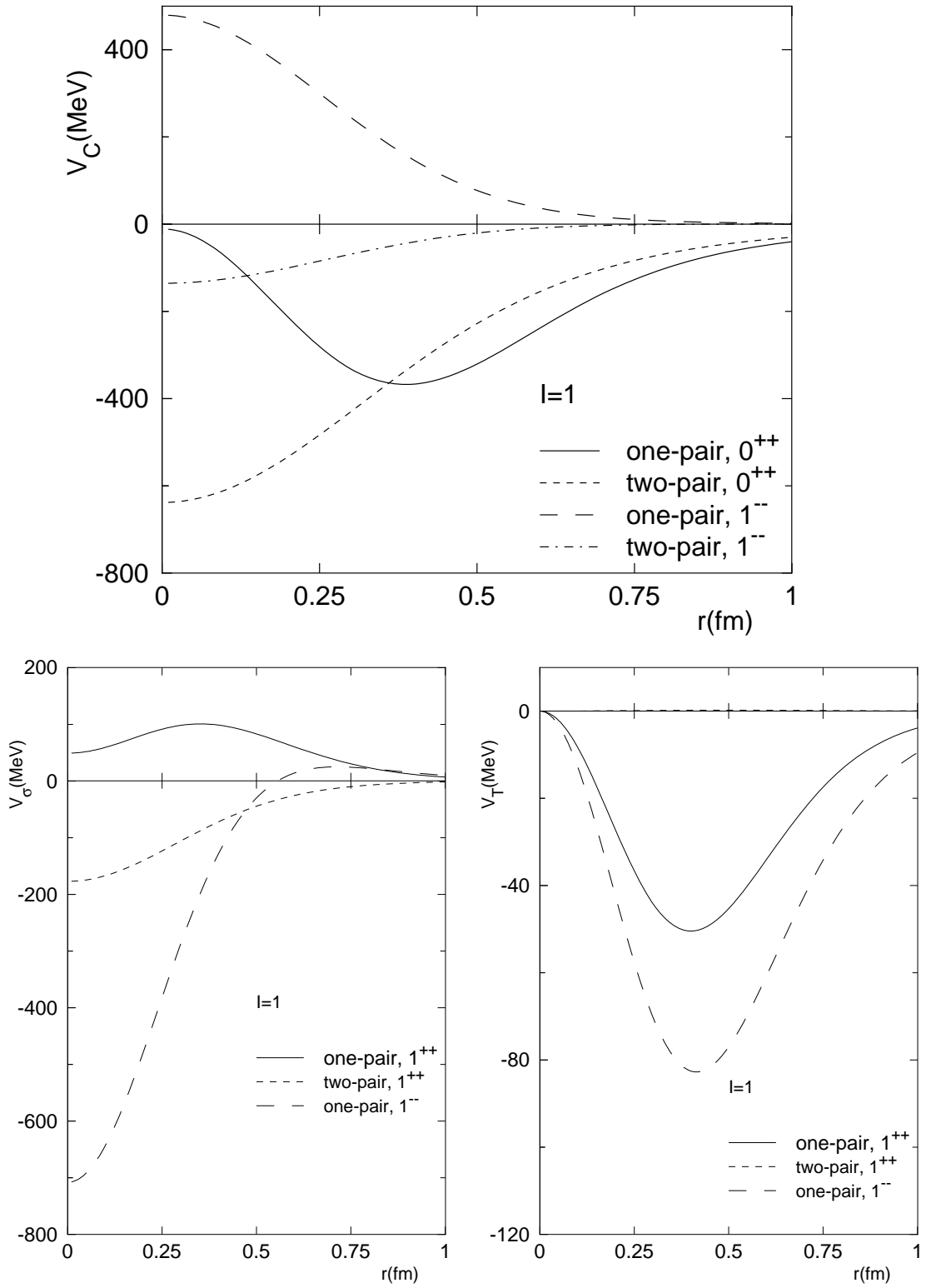
FIG. 5. continued

18

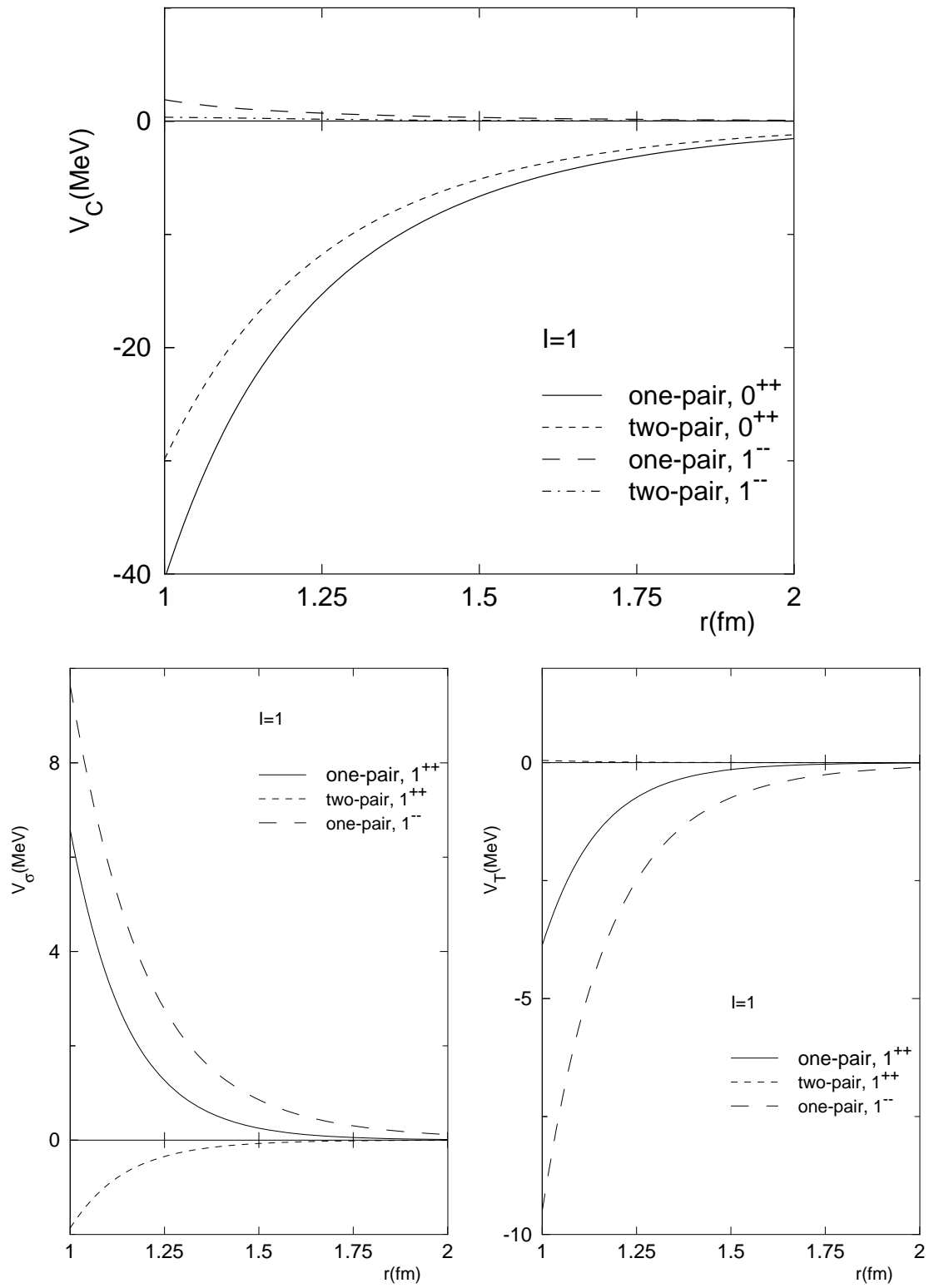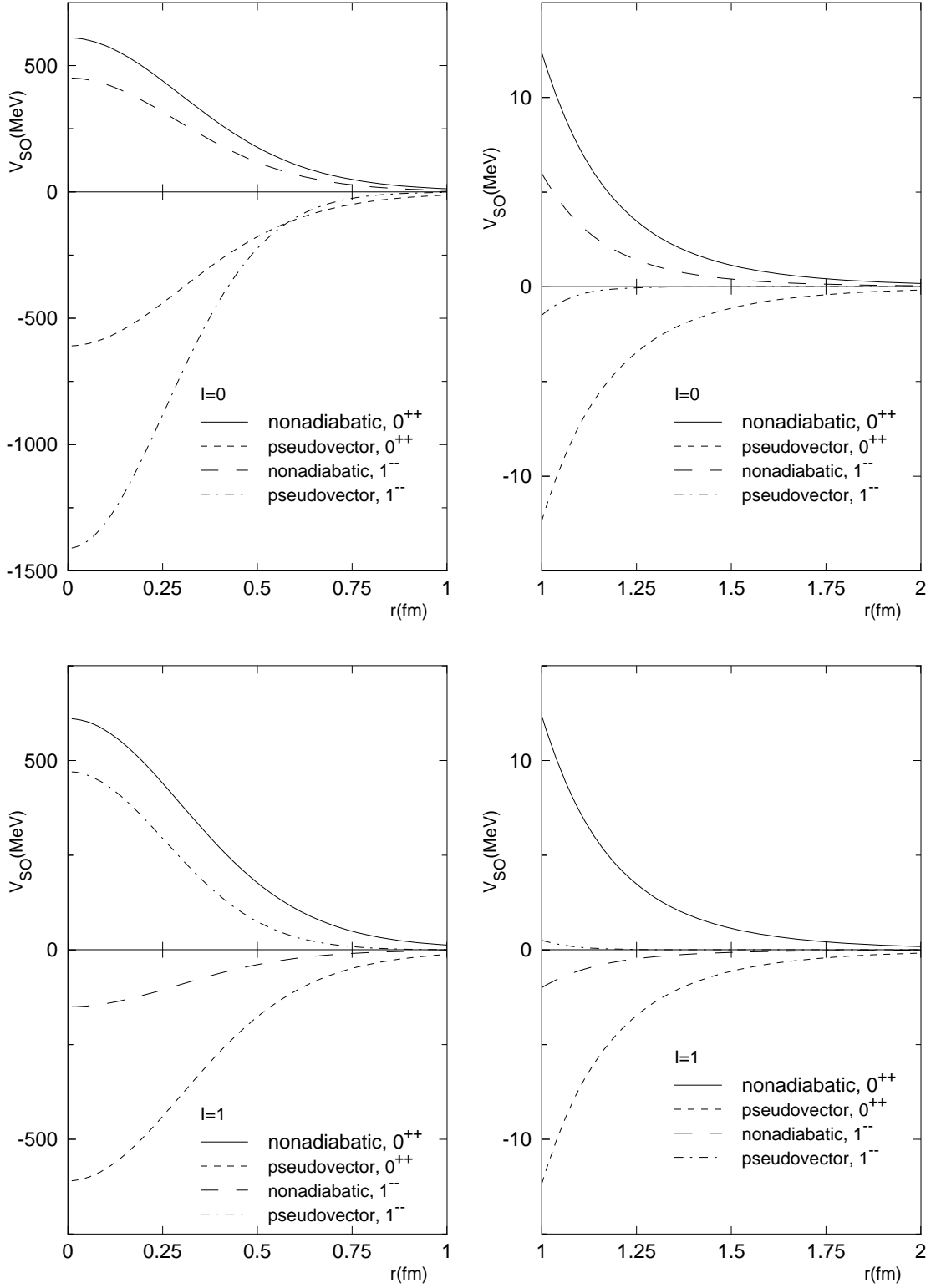FIG. 6. Same as Fig. 5, but for $I = 1$.

FIG. 6. continued

FIG. 7. Spin-orbit contributions of the one-pair 0^{++} and 1^{--} potentials for both $I = 0$ and $I = 1$. A distinction is made between the nonadiabatic and pseudovector-vertex contributions.